Columnar and surface aerosol load over the Iberian Peninsula establishing annual cycles, trends, and relationships in five geographical sectors

D. Mateos*, V.E. Cachorro, C. Toledano, M.A. Burgos, Y. Bennouna, B. Torres, D. Fuertes, R. González, C. Guirado, A. Calle and A.M. de Frutos

Grupo de Óptica Atmosférica, Facultad de Ciencias, Universidad de Valladolid, Paseo Belén 7, CP 47011, Valladolid, Spain.

*Corresponding author: mateos@goa.uva.es

Abstract

The study of atmospheric aerosol load over the Iberian Peninsula (IP) under a climatological perspective is accomplished by means of PM_{10} and AOD_{440nm} measurements from EMEP and AERONET networks, respectively, in the period 2000-2013. The PM_{10} annual cycles in five Iberian sectors show a main maximum in summer and a secondary in spring, which is only observed in the southern area for the AOD climatology. The characteristics of PM_{10}-AOD annual cycles of each geographical sector are explained by the different climatology of the air mass origins and their apportioning. The two magnitudes are correlated with a factor ranging between 20 and 90 depending on the sector. The temporal evolution of the aerosol load has shown a notable decrease in the IP since the 1980s. Statistically significant trends are obtained in the Northeastern sector with a reduction of 26% (period 1985-2000) for the total suspended particles, which continues for the PM_{10} data with a value of 35% per decade (2001-2013), and also in the whole column, 61% per decade in the AOD_{440nm} (2004-2013).

Keywords: Particulate matter; Aerosol optical depth; Aerosol Climatology; Aerosol load trend; Air mass analysis.

Highlights:

1) PM_{10} annual cycle shows two annual maxima; AOD only in the southern area

2) Air mass climatology explains the evolution of surface and columnar aerosols

3) Continuous fall in aerosol load is proved over the Iberian Peninsula (1985-2013)

1. Introduction

The effects caused by atmospheric aerosol particles on Earth's climate and radiative budget, air quality, human health and material degradation have motivated their analysis worldwide (e.g., Boucher et al., 2013, and the references therein). Climate change studies require a global and generalized aerosol characterization in order to assess its radiative forcing (direct and indirect effects; Lohmann and Feichter, 2005) and associated uncertainties. In order to successfully achieve this objective, aerosol measurements and modeling need to go together from global to regional scale. In the field of atmospheric aerosol studies, measurements based on remote sensing and "in situ" techniques have not always evolved together. Air quality and aerosol climate studies have constituted two traditional fields for aerosol studies with their specific particularities. The first one is usually linked to chemical-physical composition and pollution, while the second one is mostly related with the optical or radiative aerosol properties.

The primary element to account for the impact of the aerosol particles is their load in the atmosphere, represented by the mass concentration of particulate matter (PMx or TSP) in one case or by the aerosol optical depth (AOD) in the other one. The aerosol load in the atmosphere depends on both natural and anthropogenic emissions, atmospheric synoptic circulation patterns which govern long-range transport, local meteorology and topographical characteristics, among others. The PM_{10} (or $PM_{2.5}$) gives the particle mass concentration expressed in micrograms per unit of volume for particles with aerodynamic diameter less than 10 μm (or less than 2.5 μm). The TSP refers to the total suspended particles. Although these variables can be measured at any atmospheric altitude by airborne platforms, the existing data series refer mainly to ground-based records belonging to different air quality networks. Besides, the aerosol optical depth (AOD) represents a dimensionless parameter linked to the aerosol load in the whole atmospheric column, as an indicator of the radiation attenuation by aerosol particles.

The optical or radiative aerosol properties are measured by global world wide networks, as the AERONET (Aerosol Robotic Network, http://aeronet.gsfc.nasa.gov), or the GAW-PFR network (http://www.pmodwrc.ch/worcc). These networks are based on sun-photometer instruments which measure direct solar and diffuse sky radiation at several wavelengths, being the spectral AOD the primary key property. The AERONET project, starting in the 1990s, has been developed with the aim of monitoring the long term aerosol optical properties from ground, as well as providing a global database for the establishment of aerosol climatology, validation of satellite retrievals and aerosol models. Several local aerosol climatologies have been established based on this type of data (see, e.g., Holben et al., 2001; Dubovik et al., 2002; Toledano et al., 2007; Bovchaliuk et al., 2013). AERONET is structured as a federation of regional-national networks, among them the Iberian Network for Aerosol Measurements (RIMA,http://www.rima.uva.es), created in 2004 and managed by the Group of Atmospheric Optics, University of Valladolid (GOA-UVa). The RIMA-AERONET network ensures the provision of long-term and quality controlled data at several locations across Spain, Portugal and other countries in Europe into the AERONET-EUROPE framework.

Aerosol measurements in remote (background) sites are a useful tool to establish the aerosol long-term trends. For this purpose, the European Monitoring and Evaluation Programme (EMEP) was created as a scientifically based and policy driven program under the Convention on Long-range Transboundary Air Pollution (CLRTAP) for international co-operation. In the EMEP report of 2013 (Aas et al., 2013), the yearly evolution of PM_{10} emissions was established between 2000 and 2011 for the European continent. There are countries with a notable increase of PM_{10} emissions during this period (e.g., Belarus, Moldova, Bulgaria, and Lithuania). However, other European regions present a decrease of PM_{10} emissions (e.g., Belgium, France, The Netherlands, and UK). In particular, Spain has shown a decrease around 25%. Furthermore, the PM_{10} mass measurements from sixteen European sites have shown an average decrease of 18% per year between 2000 and

2011, which means an annual loss (in average mass concentration) of 0.29 μg m^{-3} (Aas et al., 2013). The directive 2008/50/EC of the European Parliament (May 2008) aims at reducing pollution and improving the air quality over Europe limiting the thresholds that can be reached at different time scales. For instance, to protect human health, the daily mean PM_{10} concentration must not exceed 50 μg m^{-3} more than 35 times through a year, being the annual mean limited to 40 μg m^{-3}.

The interest of the Mediterranean Basin and, particularly, Spanish region is motivated by the high PMx concentration compared to other European regions. The Mediterranean Basin is a vulnerable region in terms of the climate destabilization, which produces a more complex role of the aerosol particles in the climate system (Querol et al., 2009a). Many studies have focused on the particulate matter evolution in Spain or Western Mediterranean area (e.g., Querol et al., 2009a, 2009b; Barmpadimos et al., 2012; Salvador et al., 2012; Cusack et al., 2012; Pey et al., 2013; Gkikas et al., 2013; Bennouna et al., 2014; Notario et al., 2014). For instance, Salvador et al. (2012) have shown that the PM anthropogenic sources have decreased between 1998 and 2008 in the Madrid metropolitan area (Central Spain). For the same latitudinal belt, Notario et al. (2014) reported the weekend effect for PM_{10} data. Overall, PM concentration seems to decrease in the last years in the Iberian Peninsula (e.g., Cusack et al., 2012; Barmpadimos et al., 2012). The seasonal cycle followed by PM concentrations with large values during the warm season is shown by, e.g., Querol et al. (2009a), Kassomenos et al. (2014), and Notario et al (2014).

Several studies have dealt with the high influence played by African mineral dust events in the Mediterranean Basin (e.g., Querol et al., 2009a, 2009b; Pey et al., 2013; Gkikas et al., 2013). Overall, 15% of the PM_{10} levels over Spain is due to desert dust events (Querol et al., 2009b). Concerning human health, Reyes et al. (2014) have shown that periods under African air mass intrusions presented a significant increase in respiratory-cause admissions in hospitals of Madrid (Central Spain).

The geographical position of the Iberian Peninsula makes that this area is reached by a variety of air masses of various origins (maritime, continental and tropical, among others), with a prevalence of air masses of maritime (Atlantic) character (e.g., Valverde et al., 2014). Toledano et al. (2009) obtained, from an air mass analysis over South-western Spain, that Saharan dust intrusions are originated from North Africa as tropical continental and maritime air masses mostly in summer and late-winter/early spring. For the central area, Salvador et al. (2013) found a larger contribution of the Atlantic origin, while the Mediterranean and Continental (European) source areas seem to play a minor role. For central Spain, desert dust intrusions occur on 9% of the days between 2001 and 2008.

With this background, the aim of this study is to perform a meaningful analysis of the aerosol load over the Iberian Peninsula (IP), considering both PMx and AOD data from a climatological perspective. We are aware that the use of the term "climatology" for the aerosol data series in the IP must be taken with care. However, the existing series give a valuable view about the behavior of the annual cycles and inter-annual changes. Derived parameters as the $PM_{2.5}/PM_{10}$ ratio and the Ångström α coefficient, which provide information on the fine or coarse particle predominance, are also considered in the analysis. Particulate matter concentration (PM_{10} and $PM_{2.5}$) at the surface is obtained from the EMEP Spanish stations, while the aerosol optical depth data are taken from all the available AERONET (AErosol RObotic NETwork) Iberian sites. The analyzed period spans from 2000 to 2013 (data availability depends on the sites). The simultaneous use of the surface and columnar aerosol measurements is a suitable approach to characterize the aerosol load, but for this purpose, a detailed air mass analysis is also required. In this context, five Iberian sectors have been considered because of the observed differences among all the sites. The contribution of seven types of air masses has been evaluated. The relationship between the surface and columnar aerosol is also investigated. Finally, the study is complemented with the long-term

trends of the aerosol load in the last quarter century. The total suspended particles (TSP) in the period 1988-2000 were included to extend the analysis of surface aerosols.

This study is affordable in the Iberian Peninsula due to the large density in aerosol ground-based sites which is not easily encountered in other worldwide countries/areas. The use of geographical sectors minimizes the existence of temporal gaps in the individual data series caused by different problems. The analysis of the aerosol properties from a global perspective helps understanding the large variety and variability of aerosol conditions in the small latitudinal belt of 8º spanned by the Iberian Peninsula. Furthermore, the knowledge of the long-term trends and climatology of the aerosol load is required to implement new strategies in air quality control. In this sense, the simultaneous analysis of PMx and AOD provides a more complete characterization of the aerosol particles in the whole atmospheric column.

2. Database and methods

2.1. Data collection

The aerosol optical depth (AOD) data used in this study are collected from AERONET (AErosol RObotic NETwork) (Holben et al., 1998) in all the Iberian sites with data during, at least, one year (see Table 1 and Figure 1a). In this study, the AOD at 440nm wavelength (AOD_{440nm}) and Ångström exponent (α) are level 2.0 (quality assured) data. The radiometers placed at the Iberian Peninsula are part of RIMA and are periodically calibrated by GOA-UVA and PHOTONS-LOA[1] platforms following AERONET protocols. The estimated uncertainty is ±0.01 for AOD_{440nm}, and ±0.04 for the Ångström exponent (see, e.g., Schuster et al., 2006). The large aerosol database has been generated using the AEROPA project page, powered by CAELIS (www.caelis.uva.es). This

[1] Laboratory of Atmospheric Optics (LOA), University of Lille. PHOTONS is the name of the French network federated to AERONET and managed by LOA.

web tool offers the possibility of an easy handling of AERONET data. Furthermore, there are graph and mapping tools which are very useful in producing data quick-looks.

In order to characterize the evolution of PM over Spain, data from 15 regional background sites are obtained from EMEP database (www.emep.int). Table 2 and Figure 1a show the geographical information of the EMEP sites with PM_{10}, $PM_{2.5}$, and TSP data. The records of TSP started in the 1980s, covering a period in the Iberian Peninsula between 1985 and 2002, being replaced by PM_{10} and $PM_{2.5}$ since 2001. A complete description of the EMEP sites and the methodologies to perform PMx mass measurements has been carried out by, e.g., Querol et al. (2009a), Cusack et al. (2012), Aas et al. (2013), and references therein. The high quality of the EMEP data is assured (e.g., Pey et al., 2013).

In addition to the PMx and AOD data, other two variables are used in the analysis, which allow a better classification as a function of the aerosol size predominance. The $PM_{2.5}/PM_{10}$ ratio is a 'semi'-direct calculation of the weight of small particles (< 2.5μm) with respect to the total. Furthermore, the coarse mode ($PM_{2.5-10}$) can be estimated with the difference $PM_{10} - PM_{2.5}$. Linked to the AOD spectral shape it is defined the α Ånsgtröm exponent, which gives a quantitative idea of the particle size predominance (see e.g., Toledano et al., 2009) ranging from 0 to about 3, being small for large particles and vice versa. Therefore, the use of PM_{10}, $PM_{2.5}$, AOD_{440nm}, $PM_{2.5}/PM_{10}$ and α provides a complete database to carry out analysis in terms of aerosol load and particle size predominance at the surface and in the whole atmospheric column.

2.2. Methods

The original daily data (PMx, AOD, α, and TSP) are averaged to obtain monthly means when, at least, more than half of the days present measurement. In this way, the reliability of the monthly mean values is reinforced. In addition, annual means are evaluated only when more than 200 days

within the year have data. Seasonal analysis is performed considering: Winter (DJF), Spring (MAM), Summer (JJA), and Autumn (SON).

Monthly average data for all available PMx and TSP sites (see Table 2) are averaged to construct a data set that can be interpreted as representative for the whole country. This averaged database is referred to as "Spain" or "Spanish time series".

The seasonal cycle is removed from the data in the evaluation of the temporal trends by using the monthly anomalies. An anomaly is the difference between a particular monthly mean value and the corresponding climatological (multi-annual) monthly mean considering the whole time period analyzed. With these anomalies, the temporal trend rates are evaluated following the Sen's slope method (e.g., Sen, 1968). The significance of the results is evaluated by means of the Mann-Kendall test (e.g., Yue et al., 2002). The trend rates are obtained in the corresponding units per year for the analyzed period. We decided to present the results of this study in units 'per decade' instead of 'per year' for helping the legibility of the rates. For each trend, the *p* value and the confidence interval at 95% ($CI_{95\%}$) are also evaluated.

Finally, the air mass backward trajectories arriving at several points of the Iberian Peninsula between 2001 and 2013 have been evaluated. The HYSPLIT model (Hybrid Single-Particle Lagrangian Integrated Trajectory) version 4 (Draxler and Hess, 1998; Draxler et al., 2012) is used to compute the climatology of the 120-hour back-trajectories at three heights (500, 1500, and 3000 m a.g.l.) assuming the model vertical velocity in the calculations. In order to classify the air mass origin, seven areas or sectors around the Iberian Peninsula are considered (see Figure 1b), being the whole Iberian Peninsula considered as the "local" origin. They are similar to those used by Toledano et al. (2009). To minimize the impact of the different geographical position of each sector, we only analyze the position of each air mass between the -24 h and the -120 h of the considered date. In this way, the time spent by air masses in the arrival to the central Iberian

Peninsula is not considered in the analysis, being a more homogenous evaluation with respect to the other coastal sectors. Hence, we assume that the air masses are loaded in the previous days and not loaded in the last day. In order to assess the aerosol load contribution provided by each air mass, each daily value (of PM_{10} and AOD_{440nm}) is weighted by the number of hours over each world region. Hence, the daily aerosol load is caused by the different hours overflying the different areas. Another hypothesis is made in addition: the air masses at 500 m are assumed to produce all the concentration in surface data while those at 1500 m represent the columnar load (e.g., Toledano et al., 2007). Hence, the apportioning of each air mass can be evaluated weighting the corresponding time of flight by the daily PM and AOD values. Our approaches can be considered as adequate to analyze the differences among the five Iberian sectors. However, we are aware of the strong assumption and the uncertainty in the evaluation of the apportioning of each air mass over the surface or columnar aerosol load. With this methodology the entire Iberian Peninsula can be studied from a global viewpoint to well understand the discrepancies and similarities among the different areas.

2.3. Definition of sectors

With all the available sites (considering PM_{10} and AOD data), we have found five different sectors with different annual cycles and trends in aerosol burden (see, e.g., Figure S1). These sectors facilitate the analysis of different phenomena across the Iberian geography. Figure 1a shows the definition of the Northern (N), Northeastern (NE), Central (C), Southeastern (SE), and Southwestern (SW) sectors and the sites belonging to each one. It is worth mentioning here that for some sectors, such as the N, other classification could be possible if more sites were available in this area. The south of Spain has been divided into two different sectors since the influence of the Atlantic Ocean is clearly seen in the SW area, while the SE region is modulated by the

Mediterranean Sea. These two regions present different aerosol climatology. Furthermore, the western coast of the Iberian Peninsula may need other sector, but there is only one AERONET site, Cabo da Roca, nearby Lisbon city. Previous studies (see, e.g., Obregón et al., 2012; Mateos et al., 2014a) seem to point out a different annual cycle compared to SW and C regions. As no information on surface aerosol is available from the EMEP network, this area is not investigated in this study.

The boundaries among sectors are selected in order to group sites with similar climatology in both AOD and PMx. This is the reason why two close sites can be allocated in different sectors. For instance, this is the case for Burjassot (AOD site) and Zarra (PMx data) in the Eastern coast. The former (close to Valencia city) presents an AOD climatology similar to that of the NE sites, while Zarra site (rural background) is similar to the C sites.

To corroborate these choices, the air mass analysis has also been documented. Figure 1b shows the sectors used to classify the air masses. For some critical points, which are in the boundary between two sectors, the air mass climatology has led the final selection. For instance, site Badajoz is placed in the central sector and Zaragoza in the NE area because they have more common characteristics with those areas (see Figure S2).

3. Results and discussion

3.1. Description of the annual cycles of PM_{10}, AOD_{440nm}, $PM_{2.5}/PM_{10}$ and α

Table 3 shows the complete statistics of the daily data for the five analyzed regions. With respect to PM_{10} concentration, the North and Central areas present the lowest values (<14 μg m^{-3}), in contrast to the South (SE and SW) and Northeastern areas, which show PM_{10} means larger than 16 μg m^{-3}. The SE sector exhibits the largest daily mean concentration, about 20 μg m^{-3}. The North-

South increasing PMx gradient –already observed by, e.g., Querol et al. (2009b) in the Eastern Spanish coast–, is found for the whole Iberian Peninsula. These background aerosol concentrations are in contrast with the average about 32 μg m^{-3} reported in Madrid city (C sector) by Kassomenos et al. (2014). The North-South gradient is also shown by the mean annual net dust contribution (Querol et al., 2009b); hence the African air mass intrusions over the Iberian Peninsula enhance the differences between Northern and Southern stations. This fact also produces the existence of an increasing PMx gradient from the NW to the SE of the whole Mediterranean Basin (e.g., Pey et al., 2013).

A common feature of the Iberian regions is that the median PMx are smaller than the mean. On average, the median is 88% of the mean value, and the smallest difference between them (around 8%) is observed in NE and SW sectors. This is an indicator that high aerosol load events are frequent in the whole country, presenting a substantial influence on the annual averages. The absolute difference between the median and third quantile (Q3) is also larger than the absolute difference between the median and the first quantile (Q1). With respect to the seasonal weights to the annual mean (W_X), two different groups of sectors are identified. A notably high contribution during summer is achieved in Central and Southeastern sectors, with W_{SUM} over 35% of the total. This kind of situation is in line with the high probability of desert dust or biomass burning events, and low precipitation during summer. For these areas, the weight of winter PM_{10} concentration is below 16%. This pattern is typical of Atlantic advections and higher precipitation. This seasonal partition was also reported by Querol et al. (2009a, 2009b). However, other pattern is exhibited by the rest of sectors (N, NE, and SW). For these areas, there contribution of the four seasons is even with weights over 20% for all of them. The minimum change through the year is observed in the NE and SW sectors, with a variation of only 5% among seasons. These results based on ground-based observations are in line with those findings obtained using CALIOPE model estimations of PM levels in the Iberian Peninsula (see, e.g., Pay et al., 2012). It is worth mentioning here that the

different length of the databases can cause some influence on these results. For instance, in spite of the large database (>1700 days) used in the SW sector, this is shorter than for other regions.

Regarding the particle size predominance at the surface, the $PM_{2.5}/PM_{10}$ ratio is only obtained in the N, NE, C, and SE sectors since there is no $PM_{2.5}$ data in the EMEP network for the SW sector. The daily mean value is about 0.6 and it slightly differs among Northern and Southern sectors (10% difference). The same occurs for the median and quartile variables. Overall, fine and coarse particles are practically in similar proportion throughout the Iberian Peninsula for the average conditions throughout the year. The $PM_{2.5}/PM_{10}$ ratios are clearly affected by the aerosol type, but the average conditions cause a mixture which seems to produce similar values in the different sectors. The small differences observed in the seasonal weights (see Table 3) point out a different behavior in the northern areas compared to the central and southern sectors. However, these variations are counteracted since the mean value is practically similar for the four sectors. The seasonal and monthly variability in each sector is discussed in the following sections.

With respect to columnar aerosols, the Central sector presents the lowest mean AOD_{440nm} (~0.15), and the maximum appears in the NE sector with a value of 0.2. The N sector only has 384 days with aerosol measurements, so the conclusions drawn from this table must be taken as a preliminary result. Therefore, the central sector presents the minimum values of both the PM_{10} and AOD_{440nm}. However the largest PM_{10} average is observed in the SW area. This discrepancy can be explained by the influence of Barcelona and Valencia urban areas in the NE sector on the AOD_{440nm} values. The aerosol load for these locations may increase the mean value in relation to PM_{10} (background sites of Els Torms, Cabo de Creus, and Mahón) and in relation to the SE sector. Again, the high AOD events are modifying the climatology of the daily mean values because they cause a median below the average. The seasonal weight of the AOD_{440nm} is similar for the four sectors, with a notable increase from winter (about 16%) to summer (about 35%).

The results for PM_{10} and AOD_{440nm} reported in this study are in line with the findings obtained using CALIOPE air quality modelling system (Basart et al., 2012). They obtained for the year 2004, the PM gradients mentioned above in the Iberian Peninsula and the whole Mediterranean Basin. However, their AOD values in 2004 are more homogeneous and only the summer season presented larger loads in the southern areas with respect to the northern ones.

The size predominance in the columnar aerosol measurements is analyzed using Ångström exponent α. For the five sectors, α varies between 1.0 and 1.3, thus indicating intermediate size particles with no prevalence of fine or coarse particles, in the same way as the information obtained with the $PM_{2.5}/PM_{10}$ ratio. This information is also corroborated with the median values, which do not exhibit much difference but show that the NE sector presents the highest value (1.35). The values of the first and third quartiles are in this case better indicators of the size predominance within the sectors derived from the AOD measurements. The Q1 values are smaller than 1 for the southern sectors, while the NE and C areas still present Q1 values higher than 1. Regarding Q3, the values for these latter sectors are larger than those for the other two sectors. Hence, larger particles are more often to be expected in the SE and SW sectors, while fine particles (characteristic of, e.g., urban areas) are more frequent in the NE and C.

In order to show the seasonal distribution of these magnitudes over the Iberian Peninsula, Figure 2 displays the PM_{10} and AOD_{440nm} annual cycles in the five regions. It is worth mentioning that the y-axis is common for both variables if the AOD_{440nm} is multiplied by 100, which facilitates the comparative analysis of the annual cycle. With this approach 10 μg m^{-3} in PM_{10} would be equivalent to 0.1 in AOD_{440nm}, although this correspondence must be taken only as a proxy. The proportionality factor between both variables will be deeply discussed in section 3.3. Another issue to take into account is the different sampling of PM_{10} and AOD data, which could cause some discrepancies in the annual cycles. Hence, the evaluation of the multi-annual monthly means

was also performed using only days with coincident PM_{10} and AOD data. The results are shown in the supplementary material (see Figure S3). In that figure, the PM_{10} cycle gets modified since the AOD_{440nm} sampling is lower, but the shape of annual cycle is not substantially affected and the most relevant features, as commented in the next paragraphs, are maintained.

Some of the above mentioned characteristics for the seasonal and geographical AOD and PM_{10} distribution are again shown in Figure 2. General similarity is observed between PM_{10} and AOD_{440nm} annual cycles in the N, C, and SW sectors, while worse agreement is found in the SE (June to September) and NE (May to September) regions. Even though both AOD_{440nm} and PM_{10} express the aerosol load, these magnitudes are different and special attention must be paid to the annual cycle shapes. The most relevant difference is the annual cycle showed by the PM_{10} curve with two maxima separated by a local minimum. The main maximum occurs in July-August depending on the sector, but this maximum can be shifted to June or even September depending on the particular conditions each year. The secondary maximum takes place in March in practically all sites (see figure S1 of supplementary material); this maximum can occur between February and April, as seen in the individual years. A larger PM_{10} difference between summer and early spring periods occurs in C and SE sectors compared to the two like modes of NE sector.

Conversely, the AOD presents a more defined bell shape with maxima in the summer months, an increase from March to summer and decrease afterwards in the C and NE sectors. However, the two southern sectors exhibit the same two maxima as the PM_{10} cycle. The SW sector presents the PM_{10} secondary maximum in February and the AOD_{440nm} maximum in March; whereas this effect is seen in March-April in the SE sector with a more pronounced summer maximum of PM_{10} values compared to AOD_{440nm}. In order to understand all the features shown by the sector annual cycles, the air mass back-trajectory analysis will be deeply discussed in the next section.

Furthermore, we must call attention about other singularity presented by the AOD cycle in the SW and C sectors; this is the minimum that occurs in July which is directly linked with the general atmospheric circulation over the IP. This feature appears in the AOD and also in other columnar magnitudes such as the precipitable water vapor content (Ortiz de Galisteo et al., 2014). We must also note that in this analysis the N sector is excluded because it presents an insufficient amount of data.

About particle size predominance, α and $PM_{2.5}/PM_{10}$ annual cycles are plotted for the five sectors in Figure 3 (no PM ratio is available for the SW). The PM ratio presents a more stable behavior, while α exhibits more fluctuations. Bear in mind the different range of values of the two variables: 0-1 for the ratio and between 0 and ~2.5 for α. In spite of these considerations, α seems to be more sensitive to the particle size than the PM ratio. According to α values, there is a first impact of larger particles in March in all five sectors (although with different intensity), which is also more perceptible in the initial decrease of $PM_{2.5}/PM_{10}$ ratio in the NE, C, and SE sectors. These values in late-winter and early-spring are in coincidence with the secondary maximum observed for PM_{10} and AOD_{440nm} and also agree with the high occurrence of desert dust events over the Iberian Peninsula (Toledano et al., 2009; Salvador et al., 2013). The SE sector presents a notable seasonal cycle with α varying between 0.7 and 1.4, exhibiting a progressive increase in the aerosol size up to late summer; beyond this point the aerosol size starts to decrease. The SW, C, and NE sectors exhibit a more stable behavior through the year. Overall, high variability is observed during summer months which was also mentioned by Mateos et al. (2014a), being caused by the presence of different aerosol types such as anthropogenic, biomass burning, and mineral dust (e.g., Pérez-Ramírez et al., 2008). The large influence of maritime and desert dust aerosol (large particles) causes that α is about 1.0 in the SW sector, while α is between 1.17 and 1.40 in the C and NE areas for the 12 months. Hence, a weaker influence of desert dust is observed in these sectors in contrast to SE and SW sectors. Furthermore, there are certain months in the C sector (e.g.,

between April and July) dominated by intermediate particle size (α increases from 1.15 up to 1.32) in the column measurement, while the PM ratio at the surface points out a slightly increase of the coarse mode (the PM ratio decreases from 0.58 to 0.53). With respect to the N sector, the PM ratio shows values above 0.6 for most of the months and a remarkable minimum in November (around 0.56).

3.2. Analysis of air mass origin in the five Iberian sectors

To deeply analyze the differences observed between the aerosol load at the surface and the whole atmospheric column it is necessary to investigate the air mass climatology. As mentioned, it is considered that air masses at 500 m above ground are linked to PM observations whereas those at 1500 m are linked to the AOD measurement. With this approach, the discrepancies between the surface and the lower troposphere are highlighted. The HYSPLIT model is run at five points of the Iberian Peninsula representing the five sectors defined above. The air mass backward trajectories are evaluated for the time periods corresponding to each sector PM-AOD database. The monthly climatology of the relative frequency of seven air mass types is studied (see Figure 1b): L (local), C (continental), Me (Mediterranean), CT (continental tropical), MT (tropical maritime), MP (polar maritime), and A (Arctic) (Toledano et al., 2009). Figures 4 and 5 show the relative frequency of each air mass at 500 and 1500 m in the five sectors and the respective contribution to the monthly mean PM_{10} and AOD_{440nm}, respectively, for each air mass type.

With respect to the central sector, the main discrepancy between the PM and AOD annual cycles occurs in spring (mainly April and May). The late-spring conditions change with respect to March and all the air masses that achieve this sector have less aerosol load at the surface. The polar maritime and Arctic air masses are the only ones which notably increase its contribution in April (with respect to March). The arrival of these clean masses at the surface contrasts with the more

polluted conditions observed in the whole atmospheric column. The continental, local, and Mediterranean air masses present large AOD_{440nm} values and, therefore, increase their contribution. The reduction of the desert dust events observed in April (considering tropical maritime and continental areas) is counteracted with these increases. Therefore, the PM_{10} is diminished by the absence of desert dust episodes at ground level and the arrival of clean air masses to this sector, but the columnar aerosol load does not suffer this decrease.

Another difference in the annual cycles of both variables is the AOD_{440nm} slight decrease in May. The PM_{10} increases with respect to April. However, the climatology of the air masses at 1500 m (a.g.l.) shows that the three types (Mediterranean, local, and continental) decrease its aerosol load with respect to April, which explains this behavior. Finally, a summer local minimum in July is observed in the AOD_{440nm} cycle, which is not visible in the PM_{10} cycle. In this month, there is a notable decrease of the contribution of air masses arriving from the tropical area (i.e. desert dust intrusions). This effect, corroborated by α data (Figure 3), causes that polar maritime, local, and Arctic areas govern the climatology. This situation reverts in August and the large particles arriving from the African continent contribute to the annual PM_{10} and AOD_{440nm} maxima. The decrease of α values in August (compared to July and September) is seen as a common feature in the other four sectors (e.g., more clearly in the NE and SW areas). This effect can be understood by the strong influence of large particles in August due to the increase in the contribution of desert dust events, that can reach the Iberian Peninsula with different pathways: maritime (from SW), continental tropical (from S), and the Mediterranean Sea (from SE). By means of a cluster analysis, Salvador et al. (2013) have found a predominance (~70% of the days analyzed between 2001 and 2008) of the Atlantic origin over the central Iberian Peninsula. This figure is in line with the results obtained in our calculations for a larger period.

The area showing the largest discrepancy between the PM and AOD evolution is northeastern Iberian Peninsula. As can be expected, the air masses at 500 and 1500 m considerably differ.

There is a more even distribution of the air mass frequencies at the lower level (500 m): continental, Mediterranean, polar maritime, Arctic, and local exhibit notable influence throughout the year. In this sense, Querol et al. (2009a) pointed out based on PM data that this area suffers of higher frequency of African dust in spring-summer, and intense pollution events and sporadic dust intrusions in winter. As it is seen in Figure 4, the tropical influence is noticeable between October (annual maximum) and March. This result is in line with the previous findings of, e.g., Escudero et al. (2005), and Pey et al. (2013). However, the conditions at 1500 m (a.g.l.) are different. The role of the polar maritime air masses is the prevalent contribution, except for September, when the continental contribution is higher. In addition, the local origin plays a key role during the warm season (between May and September), when re-circulation phenomena can transport air masses with aged aerosols. These conditions and the urban background of columnar aerosol sites included in this sector (e.g., Barcelona, Valencia, and Zaragoza) can explain the large AOD values mentioned before in the annual cycle (see Figure 2) in the NE sector. There is also another discrepancy between the PM and AOD apportioning: the Saharan dust influence. As it is mentioned above, PM_{10} presents a larger contribution between October and March, while the AOD exhibits the maximum values in spring and summer months. All the described differences caused different annual cycles for the two magnitudes.

In the SE sector, the annual cycle of both variables is similar although the PM_{10} shows a larger increase during summer months. As it is shown in the air mass relative frequency, the tropical (both from maritime or continental origin) and local origins are dominant in the upper troposphere, while at the 500 m altitude the role of the former is minor and the recirculation (local), continental, and Mediterranean air masses predominate. In both cases, the relative occurrences of Arctic or polar maritime conditions fall below 50%. For the PM_{10} cycle, local and Mediterranean contributions are the most relevant, except for July when the aerosol load minimum in the Mediterranean origin is accompanied by the increase in the load of polar maritime air masses. As

it was observed for the NE, an increase in the tropical air mass intrusions occurs in October. With respect to the AOD_{440nm} contributions, polar maritime conditions lead the values in winter and spring, and local ones the rest of the year. The high relevance of the desert dust events is shown by the large contributions observed for the CT origin in spring, summer, and autumn. This African intrusion cycle follows a different pattern than for the rest of the Iberian Peninsula.

The entire eastern Iberian coast (NE and SE sectors) has been previously analyzed in a dynamical perspective (Millán et al., 1991; 1996; Gangoiti et al., 2001). These studies point out the daily process of the Iberian thermal low during the warm season. The creation of closed-loop circulations (up-slope winds, see breezes, subsidence flows) can span for several consecutive days and makes possible the transport/re-circulation of aged aerosol over the Iberian-Mediterranean coast. As this dynamical feature is a diurnal extension of the African semi-permanent low (Millán et al., 1991), some loops of this low pressure can even achieve the Peninsula as early as in February and March. This dynamical feature probably causes the large contributions of the local origin observed at the NE and SE sectors during the summer months (see Figures 4 and 5). The surrounding area of Víznar site (the only PM site in the SE sector) with the Sierra Nevada Mountains can make this effect more visible. In addition, over the entire eastern Iberian coast is common to find Mediterranean air masses that are loaded with desert dust. These air masses can arrive directly to the Iberian Peninsula or spend some time over the Mediterranean Sea (e.g., Querol et al., 2009a).

The southwestern sector presents the largest impact of the desert dust events through the year both at the surface and in the whole column. As analyzed by Toledano et al. (2007), contributions from the tropical and Mediterranean areas are associated with desert dust intrusions which modulate the aerosol annual cycle in this sector. However, their incidence on the PM and AOD data is

considerably different. The Atlantic area is clearly governing the annual cycle of the surface aerosol load, with punctual contributions (from local, Mediterranean, and tropical origins) increasing the PM_{10}. In the whole atmospheric column, the impact of the desert dust intrusions is the key issue in March, June, and August. The smaller tropical air mass occurrence in April and July also affect the AOD_{440nm} over this region. The incidence of the Mediterranean air masses (possibly loaded with aged aerosols, including dust) is notable at the surface, while its impact on the AOD_{440nm} can be considered as negligible. This fact corroborates the findings by Toledano et al. (2009) using 5 years of column aerosol data at El Arenosillo site. The spring PM_{10} minimum in April is justified by the decrease in the contributions from CT and Me origins. Conversely, the air masses at 1500 m arrive less load in May causing the slight reduction of the AOD_{440nm} with respect to April.

There is a large influence of the Arctic and sub-Arctic zones, being the predominant conditions the whole year in the N sector of the Iberian Peninsula. This scenario of the NW Atlantic advection for the northern Iberian sites was proved as the dominant conditions by Valverde et al. (2014) in two cities (Santiago de Compostela and Bilbao) between 1983 and 2012 at 1500 m. The PM_{10} values are governed by the polar maritime and Arctic air masses, particularly in spring and summer. Other types present influence in certain months, e.g., the continental origin is the second type with more contribution in December, February and March. Finally, desert dust events in this area, which can have tropical maritime origin, are observed from January to March, with less relevance for the rest of the year. The air masses at 1500 m (a.g.l.) show a different pattern. Although the dominant type is the polar maritime, the AOD_{440nm} contributions of local and continental types present larger values in February, March, and July. The tropical maritime origin has the second largest AOD contribution in May and October. Other air masses, such as Mediterranean and tropical continental, present a negligible impact on both PM_{10} and AOD_{440nm} values. Hence, the large difference between these two variables observed during summer months

in the northern sector can be understood by the air mass analysis. For instance, the continental air masses in July are loaded with small particles (see α values in Figure 3) which do not deposit and are not detectable in the PM_{10} data but increase the AOD (column value). In the other seasons, there is a good agreement between the conditions at 500 and 1500 m.

3.3. Relationship between PM_{10} and AOD_{440nm}

As it is shown until this point, there seems to exist good correspondence between columnar and surface aerosols (with some exceptions as it is the case for the NE sector). One of the applications of the PM-AOD relationship is the retrieval of PM values from AOD data and other meteorological parameters at a global scale (e.g., Lee et al., 2011; Chudnovsky et al., 2012; 2014; Sorek-Hamer et al., 2013). To go further in the connection between them, linear fits have been performed for simultaneous records of both magnitudes. Linear relationships at different time scales have been investigated. Table 4 summarizes the results obtained in this analysis for daily, monthly and yearly averages. The surface and columnar aerosol loads are differently correlated in the five geographical sectors. The largest correlation is observed in the SE sector, with correlation coefficient ranging between 0.67 (daily values) and 0.91 (yearly values). The correlation coefficients slightly decrease in the central area (0.6 and 0.73, respectively). The correlation seems to be also notable in the N sector, but the small number of available data points for this sector makes it difficult to assess any conclusion. Finally, the SW and NE sectors show the lowest correlation coefficients (< 0.52) at daily and monthly scales.

These results are in line with previous studies. For instance, Bennouna et al. (2014) obtained a correlation coefficient of 0.56 for daily PM_{10} and AOD (440nm) in Peñausende site (central Iberian sector), although the correlation results slightly better for monthly mean values. This fact is also noticeable in our results. Using a 7-day campaign in summer 2006 at El Arenosillo site

(SW Iberian sector), Estellés et al. (2012) found a correlation about 0.9 for daily mean values between AOD (500nm) and PM_{10}. Gan et al. (2014) looked for a relationship between AOD and $PM_{2.5}$ anomaly, finding correlation coefficients of 0.71 and 0.58 in the Eastern and Western US.

To provide further insight in the correlation analysis, the AOD_{440nm} data have been classified in bins of width 0.05 centered at 0.05, 0.1, etc. The $AOD_{440nm} < 0.025$ has not been considered since it is close to the AOD_{440nm} uncertainty given by AERONET. Figure 6 and Table 5 show the results of the PM_{10} vs AOD_{440nm} comparison using this approach. The large standard deviation of PM_{10} data within each AOD bin does not mask the positive correlation between AOD and PM concentration. This analysis has been limited to those bins with at least 15 values (daily means). All the linear fits exhibit high significance. The slopes of these fits can be interpreted for four different areas: a) the NE sector exhibits the weakest increasing trend with AOD; b) the N and SW sectors exhibit a slope of about 35 $\mu g\ m^{-3}$; c) the C sector presents a slope about 60 $\mu g\ m^{-3}$; and d) the SE sector presents a sharply increase of PM_{10} means with AOD. The intercept values in the linear fits indicate the existence of a background surface pollution with a zero columnar value, observing the larger intercept, the larger aerosol load conditions in the sector.

3.4. Inter-annual evolution and trends in aerosol load

The AOD trends are required to evaluate the actual impact of aerosols on solar radiation. However, the AOD series in the Iberian Peninsula started beyond 2000. Due to the agreement showed between PM_{10} and AOD_{440nm} in previous sections, the PM_{10} can be used to interpret the long-term trends of aerosol load over the Iberian Peninsula.

The PM_{10} (and $PM_{2.5}$) measurements of the EMEP network cover two different periods, 2001-2013 and 2008-2013. Before 2001, the total suspended particles (TSP) were also measured starting in 1985. Hence, this section aims to characterize the evolution of the surface aerosol load in the last quarter century. One of the motivations of this study is to support the brightening period

(increase in the solar radiation at the surface) observed in the Iberian Peninsula beyond 1980 (e.g., Sanchez-Lorenzo et al., 2013; Mateos et al., 2013; Román et al., 2014). Attending to the available measurement type, two different periods are used in this section: 1985-2000 (with TSP data) and 2001-2013 (with PM_{10} and $PM_{2.5}$ data). The four longest TSP databases are used as representative for the sector where they are placed: Noia (N), San Pablo Montes (C), Roquetas (NE), and Víznar (SE). In this case, the SW sector is not long-term covered by TSP data. To corroborate the results obtained with PM_{10} and $PM_{2.5}$, trends are also evaluated for AOD_{440nm}.

Firstly, the yearly time series of PM_{10}, AOD_{440nm}, and TSP is plotted in Figure 7 for a quick visualization of the temporal changes. A progressive decline in the aerosol load can be observed in the five regions. With respect PM_{10} and AOD_{440nm}, the yearly values at the end of the period are lower than those of early 2000s. To quantify these trends, the monthly values are used with the methodology explained in Section 2.2. Table 6 shows the results for the five Iberian regions. The temporal trends are also evaluated for the $PM_{2.5}$, coarse mode ($PM_{2.5-10}$, obtained as the difference PM_{10}-$PM_{2.5}$), and α. Overall, the aerosol load decrease over the IP since the 2000s is corroborated with the obtained rates, with a more abrupt decrease for fine particles.

These results corroborate the decreasing trend rates obtained by previous studies with shorter time periods. The temporal trend rates reported for the Peñausende site PM_{10} data are: -5 $\mu g\ m^{-3}$ per decade between 2001 and 2009 (Barmpadinos et al., 2012); and -4.2 $\mu g\ m^{-3}$ per decade between 2001 and 2011 (Bennouna et al., 2014). In Madrid (Central Spain), non-significant PM_{10} trends were obtained between 1999 and 2008 (Salvador et al., 2012). In a detailed analysis of the period 2001-2012 at nine EMEP sites in Spain, Querol et al. (2014) reported trends between -6.8 and -2.5 $\mu g\ m^{-3}$ per decade for PM_{10}. For three Iberian sites, Mateos et al. (2014c) have found a notable decrease between 20% and 50% in the AOD_{440nm} and PM_{10} between 2003 and 2012. In a global analysis of AERONET sites and using other methodology in the calculations, Li et al. (2014) have reported AOD trends in five Iberian sites placed in the NE, C, SE, and SW sectors which are

slightly smaller (ranging between no change and -0.07 AOD_{440nm}-unit per decade) than the AOD changes obtained in this study. Finally, de Meij et al. (2013) obtained a mean rate of -0.054 AOD per decade in the 2000s for Europe using 17 AERONET sites. With respect $PM_{2.5}$ trends, the rates are in line with the previous studies. For instance, Barmpadinos et al. (2012) obtained in Peñausende a rate of -4 μg m^{-3} per decade (2001-2009), and Bennouna et al. (2014) reported a rate of -3.8 μg m^{-3} per decade (2001-2011) for the same site. The $PM_{2.5}$ sector trends in Table 6 are in line with those obtained by Querol et al. (2014) in the EMEP sites between 2001 and 2012. Finally, Salvador et al., (2012) obtained a rate of -24.1% per decade in $PM_{2.5}$ for an urban background dataset in Madrid (C sector).

It is worth mentioning the considerable differences among the trends in the five sectors. As the NE and SE sectors present the largest PM_{10} and AOD_{440nm} values, their trends also have the largest rates. I.e., the larger the aerosol load was, the larger the reduction that has occurred. For instance, AOD values in the NE sectors have reduced 61% per decade in the 2004-2013 period. Note however, that the different time periods of all the databases used in the evaluation of each sector series can impact the results.

The evolution of the particle size predominance can be analyzed with the trends in α and the three PMx variables. The negative trends obtained for α are an indicator of a change in the aerosol composition. For instance, the NE sector presents the strongest change with -0.3 unit of α per decade (*p value* of 0.03). In addition, only the central sector exhibits a trend with high significance (around 94%) and a value of -0.1 unit of α per decade. The rates obtained for these two sectors agree with those presented by Li et al. (2014) in the Palencia and Barcelona sites, who justify both the AOD and α trends by the reduction of the fine mode anthropogenic emission in Europe. Furthermore, α change can also point out a progressive dominant role of large particles over the Iberian Peninsula. To verify these hypotheses, the trends of surface fine ($PM_{2.5}$) and coarse ($PM_{2.5-10}$) modes are also presented in the table. Both modes present negative rates (for those cases with *p*

value < 0.05) but the magnitude depends on the sector. The N and C areas present larger absolute (-3 μg m^{-3} per decade) and relative (around -40% per decade) decrease for the fine particles than for the coarse mode (e.g., -34% and -13% per decade in the NE and C sectors, respectively). In this case, the large particles gain weight with respect to the total and can explain the negative trend in α. The NE area exhibits the largest decrease of the $PM_{2.5}$ in the Iberian Peninsula (-5.28 μg m^{-3} per decade). However, its trend of the coarse mode presents low significance and its evolution is difficult to assess. In spite of this, the strong α fall seems to point out a relative increase of the coarse mode. Finally, the SE sector exhibits opposite behavior and the coarse mode suffers larger decrease (-4.65 μg m^{-3} and -50% per decade) than the fine mode. All these findings can be understood by the prevalence of fine/coarse particles over each region (see, e.g., Figure 3).

All the available PMx databases have been averaged to evaluate a Spanish monthly value between 1987 and 2013. With this monthly series, the annual cycle can be obtained for the TSP (1987-2000) and PM_{10} (2001-2013) values. To analyze the time series and find the months presenting a higher influence (by increasing or decreasing) on PM concentration, the monthly series is divided by the corresponding (TSP or PM_{10}) monthly climatological (multi-annual) mean. Figure 8 presents this anomaly, and some conclusions can be drawn. The majority of the monthly values present values within ±20% of the climatological mean. A common feature in the two periods is the larger values achieved at the beginning of each period in comparison with the mass concentrations at the end of them. The monthly mean values are notably larger (>20%) than the climatological means up to 1993 (TSP) and 2008 (PM_{10}). In particular, the period between September-1988 and February-1989 is the longest period with large PM values at the surface. Several years stand out because of their low PM concentration through the whole year: 1994, 1996, 2009, 2010, and 2013. These years only present three monthly means larger than the climatological mean (not exceeding +20%) and in some months the mean is as low as 50% of the climatological value. With respect to years with large PM concentrations, only 2004 and 2005

present large values through the year (only four months with low concentrations, not lower than -20% of the climatological mean). Year 2004 was highlighted by Pey et al. (2013) as one of the years with largest occurrence of severe desert dust episodes in Southern Spain. Five months (February, March, July, September, and November) exceed the monthly PM climatological value by 50%. Cachorro et al. (2008) have shown in July-2004 the strongest desert dust intrusion, mixed with smoke, ever recorded over the Iberian Peninsula using columnar aerosol measurements. This event is also visible in the PM data from Peñausende site (Bennouna et al., 2014), and it is also present in the Spanish database used in Figure 8. Furthermore, March exhibits high PM_{10} concentration in 2003 and 2004. Other two extreme peaks are observed in the Spanish database: March-2005 and December-2001. These two events present PM_{10} data larger than 50% compared to the monthly climatological mean. With respect to the lowest values at monthly scale, January-February-March-1996, January-February-2010 and February-March-2013 present consecutive months with low PM monthly mean data. Winter 2010 has been reported as one of the coldest winters, with a persistent and negative phase of NAO index that has impact on the IP (e.g., Mateos et al., 2014b).

Figure 7 also shows the yearly time series of TSP concentration in five Spanish sites (small-circle-line graphs). Four out of five sites exhibit a notable decrease in the TSP concentration with time, while only Víznar site presents a substantial increase in the TSP concentration between 1995 and 2002. To quantify these results, Table 7 presents the temporal TSP trends (using monthly values and the same methodology explained in Section 2) at the five ground-based sites and corresponding measurement periods. Although high statistical significance is not achieved in these data, a decrease in the TSP concentration is observed across Spain (with the exception of Víznar site). The most significant trend is obtained at Roquetas site (NE sector) with -11.9 $\mu g\ m^{-3}$ per decade. This rate between 1998 and 2000, which means around -26% per decade, is continued by the PM_{10} trend at site Els Torms with a decrease of -35% beyond 2001 in the same sector. The

negative TSP trend rates shown in Table 7 in Noia (N sector), and San Pablo Montes (C sector) are continued since 2001 by the PM_{10} series in the closest sites. Therefore, a reduction of particulate matter is observed in, at least, the Central, Eastern, and Northern areas of the Iberian Peninsula in the last quarter century. This relevant result can be used to interpret some of the long-term radiation trends reported for this area. For instance, Sanchez-Lorenzo et al. (2013) and Mateos et al. (2013) have shown an increase in the shortwave radiation at the surface at 13 ground-based stations between 1985 and 2010. The fall in the aerosol load reported in this study may be linked to this brightening period, although the change in cloudiness can play a notable role too (Mateos et al., 2014c). In addition, the reduction of the PM in Spain is in line with the decrease trend observed in the AOD observations starting in 1985 in central Europe (Ruckstuhl et al, 2008). Although the AOD is the most suitable parameter to analyze the radiative field, the PM data series have better sampling and are independent of cloudiness. Therefore, PM long-term trends can help to determine whether the solar radiation trends can be interpreted as a consequence of the aerosol load decrease in the atmosphere.

4. Conclusions

With the longest and most reliable information available about the aerosol load over the Iberian Peninsula, both at the surface and the whole atmospheric column, five different Iberian sectors have been established in this study. The discrepancies between surface and columnar aerosols provide an exhaustive analysis of the aerosol types achieving each sector. Data from the EMEP and AERONET networks are used in the analysis, which presents the following conclusions:

1) The PM_{10} annual cycle presents a first maximum in March (early spring), associated to large particles and a second one in summer (July or August) separated by a local minimum in April. With respect to AOD, the southern sectors (SW and SE) exhibit the same annual pattern as PM_{10}.

However, in the remaining sectors the AOD presents a more defined bell shape with maxima in summer months. Dynamical features like the Iberian thermal lows can explain the aerosol behavior through the year. Larger particles are observed in the southern area compared to the other areas of the Iberian Peninsula.

2) The differences between surface and columnar aerosols are explained by the air mass climatology within each sector. The polar maritime and Arctic air masses are proved as the main responsible of the aerosol climatology (N and C sectors). However, the eastern coast (NE and SE sectors) presents a dominant role of the Mediterranean air masses which cause different aerosol climatology with respect to the other sectors. Finally, African air mass intrusions loaded with desert dust strongly modulate the annual cycle shape in the southern area (SW and SE sectors).

3) The relationship between PM_{10} and AOD_{440nm} is proved with the sector databases. There is correlation between both variables, although this relationship is clearly affected by the meteorological and synoptic conditions. The discrepancies observed between the PM_{10} and AOD_{440nm} annual cycles are the base to understand the relationship between these two variables. Overall, the AOD_{440nm} and PM_{10} are approximately correlated by a factor between 20 and 90 in the Iberian Peninsula.

4) A clear decrease of the aerosol load over the Iberian Peninsula is observed since the 2000s in all five sectors. Both PM_{10} and AOD_{440nm} dropped in the last years. The composition of the atmospheric aerosols has also slightly changed due to the negative trends (statistically significant) in the Angstrom exponent α, and fine and coarse modes. Analyzing the total suspended particles between 1985 and 2000, a reduction of the aerosol load at the surface can be ensured during the last quarter century. For instance, a reduction of 26% in the TSP concentration is observed between 1987 and 2000 followed by a decrease in the PM_{10} of 35% (2001-2013) in the NE sector. This decrease has potential effects such as the increase of the solar radiation reaching the surface.

5) The mean data series of surface aerosol load for the Iberian Peninsula is studied between 1987 and 2013 in order to identify periods with low/high aerosol conditions. The years of 1994, 1996, 2009, 2010, and 2013 presented low concentration of surface aerosols, while 2004 and 2005 stand out because of their high concentration values.

The present study shows the aerosol climatology over the entire Iberian Peninsula. The definition of the five geographical sectors results of great relevance to well understand the long-term evolution of the aerosol load and its annual cycle. The use of the sector analysis can introduce some uncertainty regarding the behavior of each individual data set; however long gaps in the surface or columnar data are filled with other nearby sites. Therefore, a more stable database is used here. Furthermore, the complex role played by the aerosol particles in the climate system is highlighted for the "small area" of the Iberian Peninsula. We reckon that the individual analysis of the aerosol properties in each individual site is more specific but the conditions of the Iberian Peninsula (dynamics, meteorology and geography) require a global approach to correctly interpret the aerosol behavior in the Southwestern Europe, as part of the Mediterranean Basin with a strong Atlantic influence.

Acknowledgements

The authors are grateful to EMEP for providing observations from their network. Special thanks also go to NASA/GSFC, PHOTONS/LOA and RIMA/GOA staff for their long-standing collaboration and for operating and maintaining the AERONET network. Furthermore, all Principal Investigators of the Iberian sites are gratefully acknowledged for their effort in well-maintaining their sites. The research leading to these results has received funding from the European Union Seventh Framework Programme (FP7/2007-2013) under grant agreement Nr. 262254 [ACTRIS]. Financial supports from the Spanish MINECO (projects of ref. CGL2011-

23413, CGL2012-33576) are also gratefully acknowledged. We also thank the Environmental Council of the CyL Regional Government (Consejería de Medio Ambiente, Junta de Castilla y León) for supporting this research. Carlos Toledano thanks Ministerio de Ciencia e Innovación and Fondo Social Europeo for the award of a postdoctoral grant (Ramón y Cajal).

References

Aas, W., et al., 2013. Transboundary particulate matter in Europe Status report 2013. *EMEP Report, 4/2013* (Ref. O-7726), ISSN: 1504-6109 (print), 1504-6192 (online).

Barmpadimos, I., Keller, J., Oderbolz, D., Hueglin, C., Prèvôt, A.S.H., 2012. One decade of parallel fine ($PM_{2.5}$) and coarse (PM_{10}- $PM_{2.5}$) particulate matter measurements in Europe: trends and variability. Atmospheric Chemistry and Physics 12, 3189-3203, doi: 10.5194/acp-12.3189-2012.

Bassart, S., Pay, M. T., Jorba, O., Pérez, C., Jiménez-Guerrero, P., Schulz, M., Baldasano, J. M., 2012. Aerosols in the CALIOPE air quality modelling system: evaluation and analysis of PM levels, optical depths and chemical composition over Europe. Atmospheric Chemistry and Physics 12, 3363-3392, doi: 10.5194/acp-12-3363-2012.

Bennouna, Y.S., Cachorro, V., Burgos, M.A., Toledano, C., Torres, B., de Frutos, A., 2014. Relationships between columnar aerosol optical properties and surface Particulate Matter observations in north-central Spain from long-term records (2003-2011). Atmospheric Measurements Techniques Discussion, 7, 5829–5882, doi: 10.5194/amtd-7-5829-2014.

Boucher, O., et al., 2013. Clouds and Aerosols. In: Climate Change 2013: The Physical Science Basis. Contribution of Working Group I to the Fifth Assessment Report of the Intergovernmental Panel on Climate Change [Stocker, T.F., D. Qin, G.-K. Plattner, M.

Tignor, S.K. Allen, J. Boschung, A. Nauels, Y. Xia, V. Bex and P.M. Midgley (eds.)]. Cambridge University Press, Cambridge, United Kingdom and New York, NY, USA.

Bovchaliuk, A., Milinevsky, G., Danylevsky, V., Goloub, P., Dubovik, O., Holdak, A., Ducos, F., and Sosonkin, M., 2013. Variability of aerosol properties over Eastern Europe observed from ground and satellites in the period from 2003 to 2011, Atmos. Chem. Phys., 13, 6587-6602, doi:10.5194/acp-13-6587-2013.

Cachorro, V. E., Toledano, C., Prats, N., Sorribas, M., Mogo, S., Berjón, A., Torres, B., Rodrigo, R., de la Rosa, J., de Frutos, A.M., 2008. The strongest desert dust intrusion mixed with smoke over the Iberian Peninsula registered with Sun photometry. Journal of Geophysical Research 113, D14S04, doi:10.1029/2007JD009582.

Chudnovsky, A., Lee, H.J., Kostinski, A., Kotlov, T., Koutrakis, P., 2012. Prediction of daily fine particulate matter concentrations using aerosol optical depth retrievals from the geostationary operational environmental Satellite. Journal of Air and Waste Management 62 (9), 1022-1031.

Chudnosvsky, A.A., Koutrakis, P., Kloog, I., Melly, S., Nordio, F., Lyapustin, A., Wang, Y., Schwartz, J., 2014. Fine particulate matter predictions using high resolution Aerosol Optical Depth (AOD) retrievals. Atmospheric Environment 89, 189-198.

Cusack, M., Alastuey, A., Pérez, N., Pey, J., Querol, X., 2012. Trends of particulate matter ($PM_{2.5}$) and chemical composition at a regional site in the Western Mediterranean over the last nine years (2002-2010). Atmospheric Environment 12, 8341-8357, doi: 10.5194/acp-12-8341-2012.

Draxler, R., Hess, G.D., 1998. An overview of the HYSPLIT4 modelling system for trajectories, dispersion and deposition. Australian Meteorological Magazine 47, 295–308.

Draxler, R.A., Stunder, B., Rolph, G., Stein, A., Taylor, A., 2012. HYSPLIT4 User's Guide. Air Resources Laboratory, National Oceanic and Atmospheric Administration (NOAA), Silver Spring, MD.

Dubovik, O., Holben, B.N., Eck, T.F., Smirnov, A., Kaufman, Y.J., King, M.D. Tanre, Slutsker, I., 2002. Variability of absorption and optical properties of key aerosol types observed in worldwide locations. Journal of the Atmospheric Sciences 59, 590-608.

Escudero, M., Castillo, S., Querol, X., Avila, A., Alarcón, M., Viana, M.M., Alastuey, A., Cuevas, E., Rodríguez, S., 2005. Wet and dry African dust episodes over eastern Spain. Journal of Geohpysical Research 110, D18S08, doi: 10.1029/2004JD004731.

Estellés, V., et al. (2012), Study of the correlation between columnar aerosol burden, suspended matter at ground and chemical components in a background European environment, J. Geophys. Res., 117, D04201, doi:10.1029/2011JD016356.

Gan, C.M., Pleim, J., Marthur, R., Hogrefe, C., Long, C.N., Xing, J., Roselle, S., Wei, C., 2014. Assessment of the effect of air pollution controls on trends in shortwave radiation over the United States from 1995 through 2010 from multiple observation networks, Atmospheric Chemistry and Physics 14, 1701-1715, doi: 10.5194/acp-14-1701-2014.

Gangoiti, G., Millán, M. M., Salvador, R., Mantilla, E., 2001. Long-range transport and re-circulation ofpollutants in the western Mediterranean during the project Regional Cycles of Air Pollution in the West-Central Mediterranean Area. Atmospheric Environment 35, 6267-6276.

Gkikas, A., Hatzianastassiou, N., Mihalopoulos, M., Katsoulis, V., Kazadzis, S., Pey, J., Querol, X., Torres, O., 2013. The regime of intense desert dust episodes in the Mediterranean based

on contemporary satellite observations and ground measurements. Atmospheric Chemistry and Physics 13, 12,135–12,154, doi:10.5194/acp-13-12135-2013.

Holben, B.N., et al., 1998. AERONET – A federated instrument network and data archive for aerosol characterization. Remote Sensing of Environment 66, 1–16.

Holben, B. N., et al., 2001. An emerging ground-based aerosol climatology: Aerosol optical depth from AERONET, Journal of Geophysical Research 106(D11), 12067–12097, doi:10.1029/2001JD900014.

Kassomenos, P.A., Vardoulakis, S., Chaloulakou, A., Paschalidou, A.K., Grivas, G., Borge, R., Lumbreras, J., 2014. Study of PM_{10} and $PM_{2.5}$ levels in three European cities: Analysis of intra and inter urban variations. Atmospheric Environment 87, 153-163.

Lee, H.J., Liu, Y., Coull, B.A., Schwartz, J., Koutrakis, P., 2011. A novel calibration approach of MODIS AOD data to predict PM2.5 concentrations. Atmospheric Chemistry Physics 11, 7991-8002.

Li, J., Carlson, B.E., Dubovik, O., Lacis, A.A., 2014. Recent trends in aerosol optical properties derived from AERONET measurements. Atmospheric Chemistry Physics 14, 12271-12289, doi:10.5194/acp-14-12271-2014

Lohmann, U., Feichter, J., 2005. Global indirect aerosol effects: a review, Atmospheric Chemistry Physics 5, 715-737, doi:10.5194/acp-5-715-2005.

Mateos, D., Antón, M., Sanchez-Lorenzo, A., Calbó, J., Wild, M., 2013. Long-term changes in the radiative effects of aerosols and clouds in a mid-latitude region (1985–2010). Global and Planetary Change 111, 288-295.

Mateos, D., Antón, M., Toledano, C., Cachorro, V.E., Alados-Arboledas, L., Sorribas, M., Costa, M.J., Baldasano, J.M., 2014a. Aerosol radiative effects in the ultraviolet, visible, and near-infrared spectral ranges using long-term aerosol data series over the Iberian Peninsula. Atmospheric Chemistry and Physics 14, 13497-13514, doi:10.5194/acp-14-13497-2014.

Mateos, D., Antón, M., Sáenz, G., Bañón, M., Vilaplana, J.M., García, J.A., 2014b. Dynamical and temporal characterization of the total ozone column over Spain. Climate Dynamics, doi: 10.1007/s00382-014-2223-4.

Mateos, D., Sanchez-Lorenzo, A., Antón, M., Cachorro, V.E., Calbó, J., Costa, M.J., Torres, B., Wild, M., 2014c. Quantifying the respective roles of aerosols and clouds in the strong brightening since the early 2000s over the Iberian Peninsula. Journal of Geophysical Research Atmospheres 119, 10,382–10,393, doi:10.1002/2014JD022076.

De Meij, A., Pozzer, A., Lelieveld, J., 2012. Trend analysis in aerosol optical depths and pollutant emission estimates between 2000 and 2009. Atmospheric Environment 51, 75-85, doi:10.1016/j.atmosenv.2012.01.059.

Millán, M., Artiñano, B., Alonso, L., Navazo, M., Castro, M., 1991. The effect of meso-scale flows on regional and long-range atmospheric transport in the western Mediterranean área. Atmospheric Environment 25A, 949-963.

Millán, M., Salvador, R., Mantilla, E., Artiñano, B., 1996. Meteorology and photochemical air pollution in Southern Europe: Experimental results from EC research projects. Atmospheric Environment 30(12), 1909-1924.

Notario, A., Adame, J.A., Bravo, I., Cuevas, C.A., Aranda, A., Díaz-de-Mera, Y., Rodríguez, A., 2014. Air pollution in the plateau of the Iberian Peninsula. Atmospheric Research 145-146, 92-104.

Obregón, M.A., Pereira, S., Wagner, F., Serrano, A., Cancillo, M.L., Silva, M.A., 2012. Regional differences of column aerosol parameters in western Iberian Peninsula. Atmospheric Environment 62, 208-219.

Ortiz de Galisteo, J.P., Bennouna, Y., Toledano, C., Cachorro, V., Romero, P., Andrés, M.I., and Torres, B., 2013. Analysis of the annual cycle of the precipitable water vapour over Spain from 10-year homogenized series of GPS data. Quarterly Journal of Royal Meteorological Society 140, 397–406, doi: 10.1002/qj.2146.

Pay, M.T., Jiménez-Guerrero, P., Jorba, O., Basart, S., Querol, X., Pandolfi, M., and Baldasano, J.M., 2012. Spatio-temporal variability of concentrations and speciation of particulate matter across Spain in the CALIOPE modeling system. Atmospheric Environment 46, 376-396, doi:10.1016/j.atmosenv.2011.09.049.

Pérez-Ramírez, D., Aceituno, J., Ruiz, B., Olmo, F.J., and Alados-Arboledas, L., 2008. Development and calibration of a star photometer to measure the aerosol optical depth: Smoke observations at a high mountain site. Atmospheric Environment 42, 2733–2738.

Pey, J., Querol, X., Alastuey, A., Forastiere, F., Stafoggia, M., 2013. African dust outbreaks over the Mediterranean Basin during 2001-2011: PM_{10} concentrations, phenomenology and trends, and its relation with synoptic and mesoscale meteorology. Atmospheric Chemistry Physics 13, 1395-1410, doi:10.5194/acp-13-1395-2013.

Querol, X., Pey, J., Pandolfi, M., Alastuey, A., Cusack, M., Pérez, N., Moreno, T., Viana, M., Mihalopoulos, N., Kallos, G., Kleanthous, S., 2009a. African dust contributions to mean ambien PM_{10} mass-levels across the Mediterranean Basin. Atmospheric Environment 43, 4266-4277, doi: 10.1016/j.atmosenv.2009.06.013.

Querol, X., Alastuey, A., Pey, J., Cusack, M., Pérez, N., Mihalopoulos, N., Theodosi, C., Gerasopoulus, E., Kubilay, N., Koçak, M., 2009b. Variability in regional background aerosols within the Mediterranean. Atmospheric Chemistry Physics 9, 4575-4591.

Querol, X., et al., 2014. 2001-2012 trends on air quality in Spain, Science of Total Environment 490, 957-969.

Reyes, M., Díaz, J., Tobias, A., Montero, J.C., Linares, C., 2014. Impact of Saharan dust particles on hospital admissions in Madrid (Spain). International Journal of Environmental Health Research 24, 63-72, doi: 10.1080/09603123.2013.782604.

Román, R., Bilbao, J., de Miguel, A., 2014. Reconstruction of six decades of daily total solar shortwave irradiation in the Iberian Peninsula using sunshine duration records, Atmospheric Environment 99, 41-50.

Ruckstuhl, C., et al., 2008. Aerosol and cloud effects on solar brightening and the recent rapid warming, Geophysical Research Letters 35, L12708, doi:10.1029/2008GL034228.

Salvador, P., Artiñano, B., Viana, M., Alastuey, A., Querol, X., 2012. Evaluation of the changes in the Madrid metropolitan area influencing air quality: Analysis of 1999-2008 temporal trend of particular matter. Atmospheric Environment 57, 175-185, doi: 10.1016/j.atmosenv.2012.04.026.

Salvador, P., Artiñano, B., Molero, F., Viana, M., Pey, J., Alastuey, A., Querol, X., 2013. African dust contribution to ambient aerosol levels across central Spain: Characterization of long-range tansport episodes of desert dust. Atmospheric Research 127, 117-129, doi: 10.1016/j.atmosres.2011.12.011.

Sanchez-Lorenzo, A., Calbó, J., Wild, M., 2013. Global and diffuse solar radiation in Spain: Building a homogeneous dataset and assessing trends. Global and Planetary Change 100, 343-352.

Schuster, G.L., Dubovik, O., Holben, B.N., 2006. Ångström exponent and bimodal aerosol size distributions. Journal of Geophysical Research 111, D07207.

Sen, P.K., 1968, Estimates of the Regression Coefficient Based on Kendall's Tau, Journal of the American Statistical Association 63, 1379-1389, doi:10.1080/01621459.1968.10480934.

Sorek-Hamer, M., Strawa, A.W., Chatfield, R.B., Esswein, R., Cohen, A., Broday, D.M., 2013. Improved retrieval of $PM_{2.5}$ from satellite data products using non-linear methods. Environmental Pollution 182, 417-423, doi: 10.1016/j.envpol.2013.08.002.

Toledano, C., Cachorro, V.E., Berjon, A., de Frutos, A.M., Sorribas, M., de la Morena, B., Goloub, P., 2007. Aerosol optical depth and Ångström exponent climatology at El Arenosillo AERONET site (Huelva, Spain). Quarterly Journal of the Royal Meteorological Society133, 795-807.

Toledano, C., Cachorro, V.E., de Frutos, A.M., Torres, B., Berjón, A., Sorribas, M., Stone, R.S., 2009. Airmass classification and analysis of aerosol types at El Arenosillo (Spain). Journal of Applied Meteorology and Climatology 48, 962-981, doi: 10.1175/2008JAMC2006.1

Valverde, V., Pay, M.T., Baldasano, J.M., 2014. Circulation-type classification derived on a climatic basis to study air quality dynamics over the Iberian Peninsula. International Journal of Climatology, doi: 10.1002/joc.4179.

Yue, S., Pilon, P., Phinney, B, and Cavadias, C., 2002. The influence of autocorrelation on the ability to detect trend in hydrological series, Hydrological Processes 16, 1807-1829, doi: 10.1002/hyp.1095.

Tables

Table 1. Information of the AERONET-Europe sites used in this study and the number of daily data (n) used from each site.

Sector	Site (number in Figure 1)	Latitude (ºN)	Longitude (ºE)	Altitude (m a.s.l.)	Time Period	n
N	Coruña (1)	43.37	-8.42	67	2012-2013	384
NE	Montsec (2)	42.05	0.73	1574	2011-2013	383
	Zaragoza (6)	41.63	-0.88	250	2012-2013	361
	Barcelona (7)	41.39	2.12	125	2004-2013	2114
	Burjassot (10)	39.51	-0.42	30	2007-2013	1506
	Palma de Mallorca (9)	39.55	2.63	10	2011-2013	567
C	Autilla (3)	42.00	-4.60	873	2007-2013	1113
	Palencia (4)	41.99	-4.52	750	2003-2013	1929
	Valladolid (5)	41.66	-4.71	705	2012-2013	187
	Madrid (8)	40.45	-3.72	680	2012-2013	330
	Cáceres (11)	39.48	-6.34	397	2005-2012	1421
	Badajoz (12)	38.88	-7.01	186	2012-2013	232
	Évora (14)	38.57	-7.91	293	2003-2013	2448
SE	Murcia (15)	38.00	-1.17	69	2012-2013	310
	Granada (16)	37.16	-3.61	680	2004-2013	1789
	Cerro Poyos (17)	37.11	-3.49	1830	2012-2013	254
	Tabernas PSA-DLR (19)	37.09	-2.36	500	2011-2013	652
	Málaga (22)	36.72	-4.48	40	2009-2013	1359
SW	El Arenosillo (18)	37.10	-6.73	45	2000-2010	2404
	SAGRES (20)	37.05	-8.87	26	2010-2012	339
	Huelva (21)	37.02	-6.57	25	2010-2013	990

Table 2. Information of the EMEP Spanish sites used in this study.

Sector	Station	Latitude (ºN)	Longitude (ºE)	Altitude (m a.s.l.)	Period PM_{10}	Period $PM_{2.5}$	Period TSP
N	Niembro	43.44	-4.85	134	2001-2013	2001-2013	-
	O Saviñao	43.23	-7.70	506	2001-2013	2001-2013	-
	Noia	42.73	-8.92	683	2008-2013	-	1993-2000
NE	Cabo_de_Creus	42.32	3.32	23	2001-2013	2001-2013	-
	Els_Torms	41.40	0.72	470	2001-2013	2001-2013	-
	Roquetas	40.82	0.49	44	-	-	1987-2000
	Mahon	39.87	4.32	78	2008-2013	2012-2013	-
C	Logroño	42.46	-2.50	445	-	-	1988-2000
	Peñausende	41.28	-5.87	985	2001-2013	2001-2013	-
	Campisabalos	41.28	-3.14	1360	2001-2013	2001-2013	-
	San Pablo Montes	39.55	-4.35	917	2008-2013	2008-2013	1985-2000
	Zarra	39.09	-1.10	885	2001-2013	2001-2013	-
	Barcarrota	38.48	-6.92	393	2001-2013	2001-2013	-
SE	Víznar	37.23	-3.53	1265	2001-2013	2001-2013	1995-2002
SW	Doñana	37.03	-6.33	5	2008-2013	-	-

Table 3. Statistics of daily PM_{10} (in μg m^{-3}), $PM_{2.5}/PM_{10}$, AOD_{440nm}, and α at the five Iberian sectors. Legend: n (number of data), SD (standard deviation), md (median), Q1 (first quartile), Q3 (third quartile), and WX is the weight of winter (X = WIN), spring (X= SPR), summer (X = SUM), and autumn (X = AUT) with respect to the mean value.

Variable	Sector	n	Mean	SD	md	Q1	Q3	W_{WIN}	W_{SPR}	W_{SUM}	W_{AUT}
PM_{10}	N	4640	13.9	8.2	12	8.5	17	20.9	27.3	27.7	24.1
	NE	4649	17.3	7.6	16	12.5	20.5	22.2	25.5	27.7	24.6
	C	4685	12.9	8.9	11	7.0	16.4	15.7	23.5	36.5	24.3
	SE	4345	19.5	16	16	9.0	25	14.6	23.1	39.3	23.0
	SW	1771	16.3	9.4	15	11.0	20	22.3	25.5	27.1	25.1
AOD_{440nm}	N	384	0.15	0.1	0.12	0.09	0.17	12.4	31.9	39.4	16.3
	NE	2367	0.20	0.1	0.18	0.10	0.27	16.9	27.7	33.5	21.9
	C	3385	0.15	0.1	0.12	0.08	0.18	16.5	27.4	35.5	20.6
	SE	2428	0.18	0.1	0.15	0.10	0.23	14.5	25.2	39.9	20.5
	SW	3613	0.16	0.1	0.13	0.09	0.2	16.1	26.0	35.3	22.6
$PM_{2.5}/PM_{10}$	N	4566	0.63	0.2	0.62	0.48	0.75	23.3	26.0	26.7	24.0
	NE	4588	0.57	0.2	0.56	0.43	0.68	24.5	25.7	26.0	23.7
	C	4683	0.58	0.1	0.57	0.49	0.67	26.3	25.9	24.1	23.7
	SE	4015	0.57	0.2	0.56	0.46	0.67	26.4	25.0	23.8	24.8
	SW	0	-	-	-	-	-	-	-	-	-
α	N	384	1.0	0.4	0.98	0.72	1.24	17.4	24.6	36.9	21.1
	NE	2367	1.3	0.4	1.35	1.10	1.56	26.7	25.8	25.5	22.1
	C	3385	1.2	0.3	1.27	1.02	1.47	22.6	24.2	29.4	23.8
	SE	2428	1.0	0.4	1.04	0.73	1.31	26.1	25.5	24.8	23.6
	SW	3613	1.0	0.4	1.02	0.69	1.29	21.3	22.4	31.7	24.6

Table 4. Correlation coefficient (r), 95% confidence interval (CI), and number of data (n) of the PM_{10} vs AOD_{440nm} relationships in the five Iberian regions. Only r data with p value ≤ 0.05 are shown.

Time scale	Variable	N	NE	C	SE	SW
Daily	r	0.59	0.42	0.6	0.67	0.37
	CI	(0.53,0.66)	(0.39,0.46)	(0.58,0.62)	(0.64,0.69)	(0.32,0.42)
	n	384	2363	3385	2233	1274
Monthly	r	0.75	0.47	0.78	0.86	0.52
	CI	(0.49,0.89)	(0.31,0.61)	(0.71,0.84)	(0.79,0.9)	(0.32,0.68)
	n	23	104	127	97	65
Yearly	r	-	-	0.73	0.91	-
	CI	-	-	(0.23,0.92)	(0.62,0.98)	-
	n	2	10	11	9	6

Table 5. Statistics of the linear relationships (see Figure 6): $PM_{10} = a + b\ AOD_{440nm}$.

Sector	a (μg m^{-3})	b (μg m^{-3})	r	CI	p
N	7.53	35.95	0.94	(0.54, 0.99)	<0.001
NE	11.65	22.01	0.99	(0.95, 1)	<0.001
C	4.60	57.77	0.97	(0.89, 0.99)	<0.001
SE	3.61	86.99	1	(0.98, 1)	<0.001
SW	11.44	37.93	0.99	(0.94, 1)	<0.001

Table 6. Temporal trends of PM_{10} (μg m^{-3} per decade), AOD_{440nm} (unit of AOD_{440nm} per decade), $PM_{2.5}$ (μg m^{-3} per decade), coarse $PM_{2.5-10}$(PM_{10}-$PM_{2.5,}$ μg m^{-3} per decade), and α (unit of α per decade).

Variable	Sector	trend	*p* value	CI	relative trend (% per decade)	Time Period
PM_{10}	N	-5.6	<0.001	[-6.95,-4.26]	-40.25	2001-2013
	NE	-4.05	<0.001	[-5.3,-2.76]	-23.42	2001-2013
	C	-3.92	<0.001	[-5.02,-2.79]	-30.55	2001-2013
	SE	-6.7	<0.001	[-8.54,-4.88]	-34.8	2001-2013
	SW	-1.58	0.63	[-4.87,2.3]	-9.56	2008-2013
AOD_{440nm}	N	x	x	x	x	2012-2013
	NE	-0.12	<0.001	[-0.15,-0.1]	-60.96	2004-2013
	C	-0.04	<0.001	[-0.06,-0.03]	-28.19	2003-2013
	SE	-0.07	<0.001	[-0.1,-0.04]	-40.47	2004-2013
	SW	-0.03	<0.001	[-0.05,-0.02]	-18.53	2000-2013
$PM_{2.5}$	N	-3.17	<0.001	[-4.05,-2.35]	-36.33	2001-2013
	NE	-5.28	<0.001	[-6.18,-4.37]	-53.57	2001-2013
	C	-3.27	<0.001	[-3.96,-2.58]	-45.95	2001-2013
	SE	-1.6	0.001	[-2.43,-0.74]	-15.99	2001-2013
	SW	x	x	x	x	-
$PM_{2.5-10}$*	N	-1.89	<0.001	[-2.58,-1.21]	-34.33	2001-2013
	NE	0.15	0.85	[-0.53,0.76]	2.02	2001-2013
	C	-0.76	0.02	[-1.36,-0.15]	-13.22	2001-2013
	SE	-4.65	<0.001	[-6.02,-3.47]	-48.65	2001-2013
	SW	x	x	x	x	-
α	N	x	x	x	x	2012-2013
	NE	-0.31	0.03	[-0.44,-0.17]	-23.47	2004-2013
	C	-0.10	0.06	[-0.18,-0.01]	-8.25	2003-2013
	SE	-0.11	0.48	[-0.28,0.06]	-10.6	2004-2013
	SW	-0.06	0.96	[-0.17,0.05]	-5.96	2000-2013

* The NE database only englobes Els Torms and Cabo de Creus sites. The two years (2012-2013) of PM2.5 data in Mahon site cause a stilted behavior.

Table 7. Absolute (relative) temporal TSP trends in μg m^{-3} per decade (% per decade) at four sites. The PM_{10} relative trend (% per decade) is given for the closest EMEP site with long-term data.

Station / Sector	TSP trends	*p* value	Interval	Time-period	PM_{10} trend (2001-2013)
Noia / N	-0.2 (-1.1)	0.85	[-0.8,0.7]	1993-2000	-37.1 (O Saviñao)
Roquetas / NE	-11.9 (-25.9)	<0.001	[-1.7,-0.7]	1987-2000	-35.3 (Els Torms)
San Pablo Montes / CE	-2.7 (-12.1)	0.25	[0.5,-0.1]	1985-2000	-28.2 (Zarra)
Víznar / SE	18.3 (50.3)	0.01	[0.8,2.9]	1995-2002	-31.6 (Víznar)

Figures

Figure 1

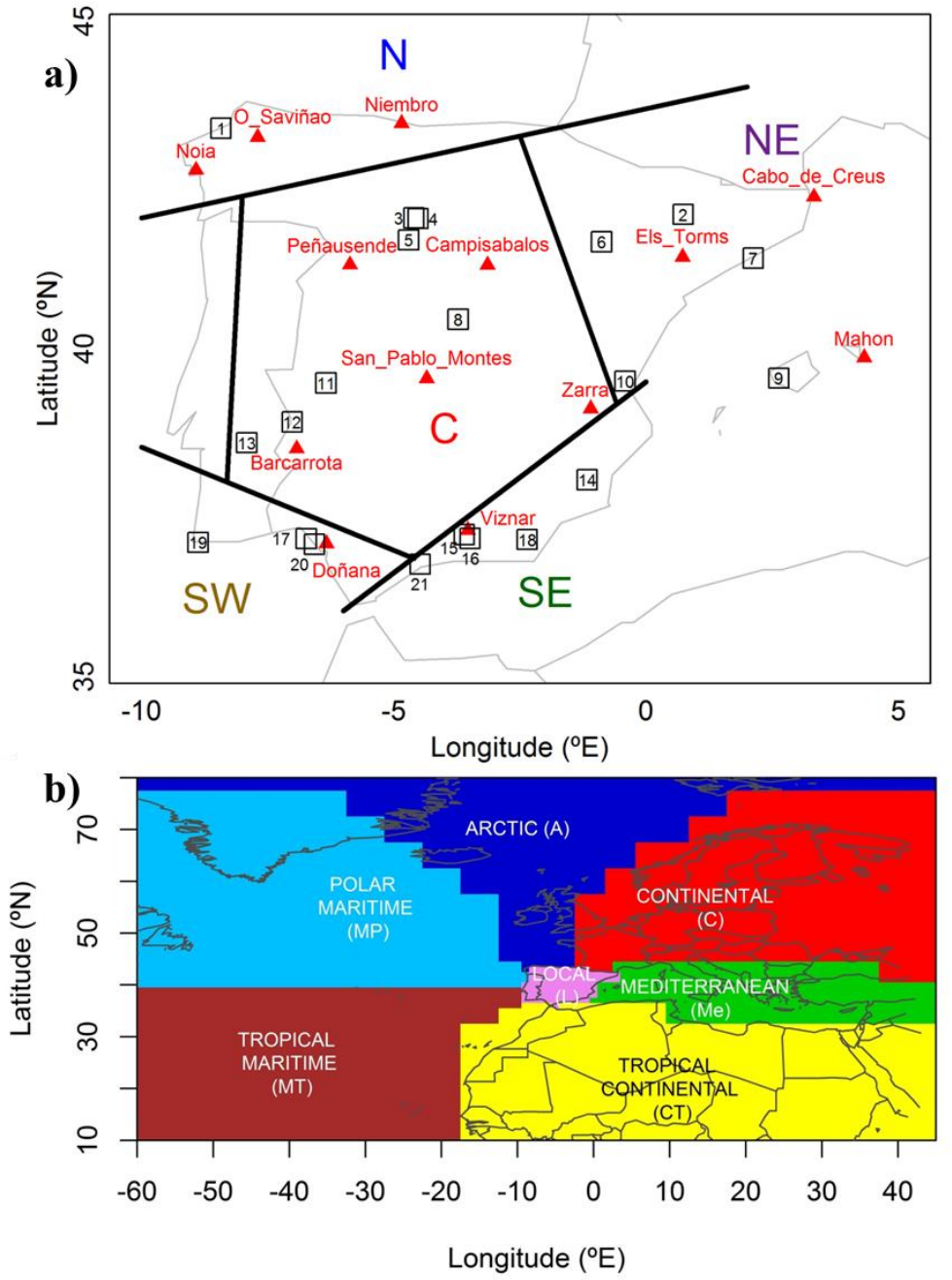

Figure 1. a) Geographical position of the EMEP (with PM_{10} data, solid triangles) and AERONET-Europe (open diamonds) sites used in this study. The numbers of AERONET sites correspond to those explained in Table 1. The definition of the five sectors in which the Iberian Peninsula is divided in this study, is also given. b) Classification grid (sectors) used in the air mass analysis.

Figure 2

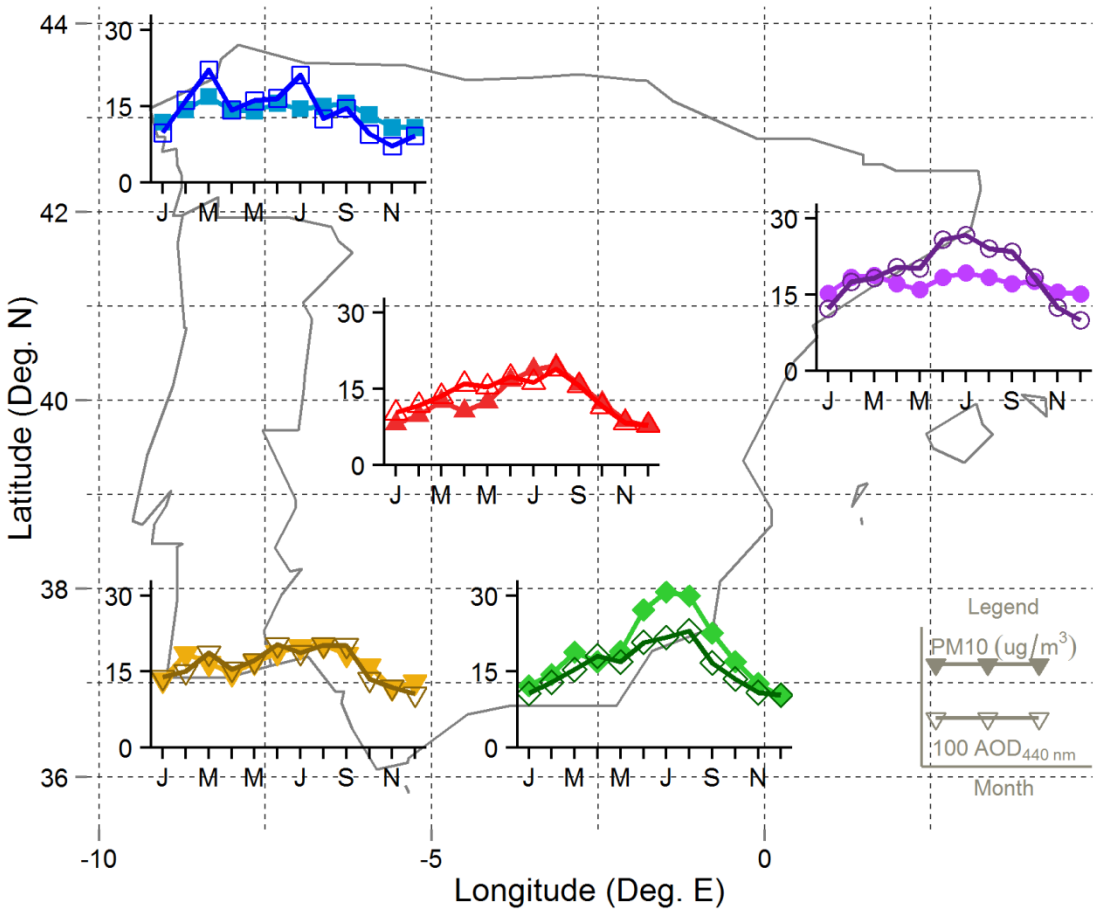

Figure 2. Annual cycles of PM_{10} (in µg m^{-3}, solid symbols) and AOD_{440nm} (plotted as 100 * AOD_{440nm}, open symbols) at the five Iberian sectors defined in Figure 1.

Figure 3

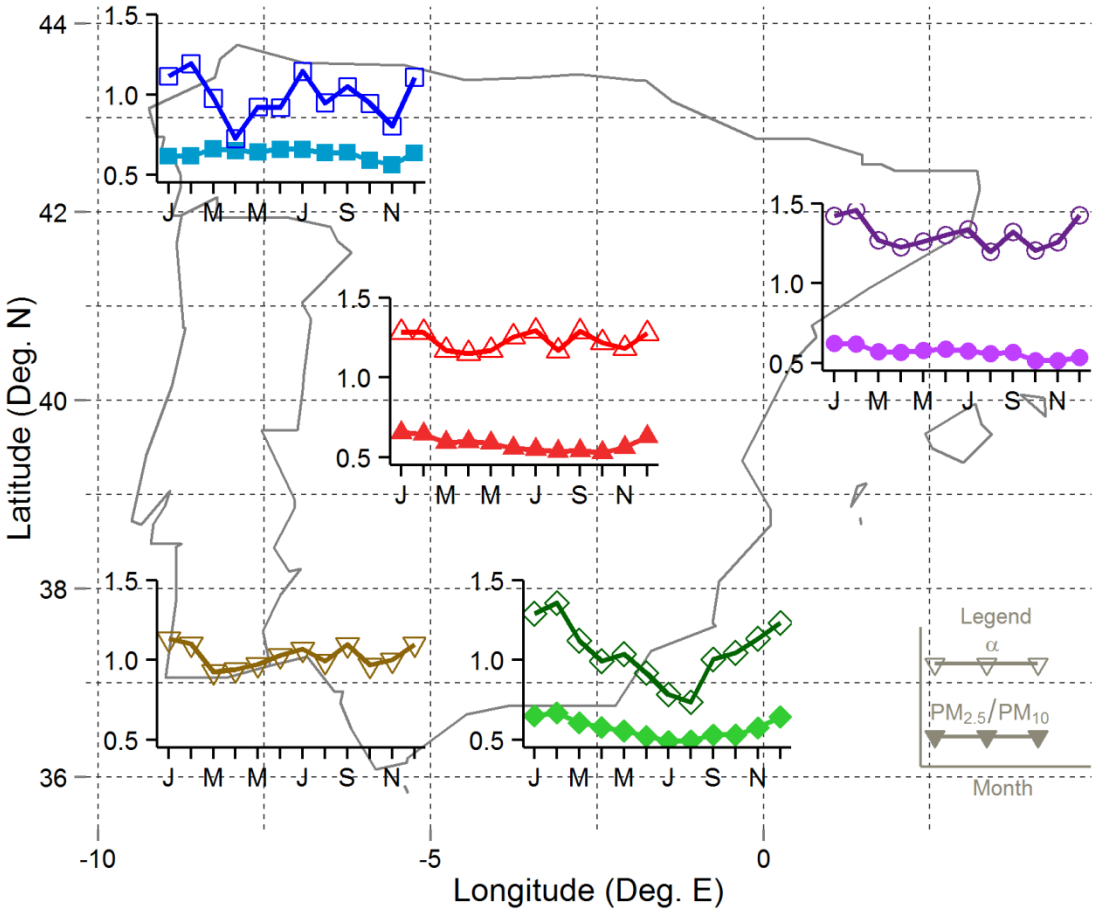

Figure 3. Annual cycles of $PM_{2.5}/PM_{10}$ (solid symbols) and α (open symbols) at the five Iberian sectors defined in Figure 1.

Figure 4

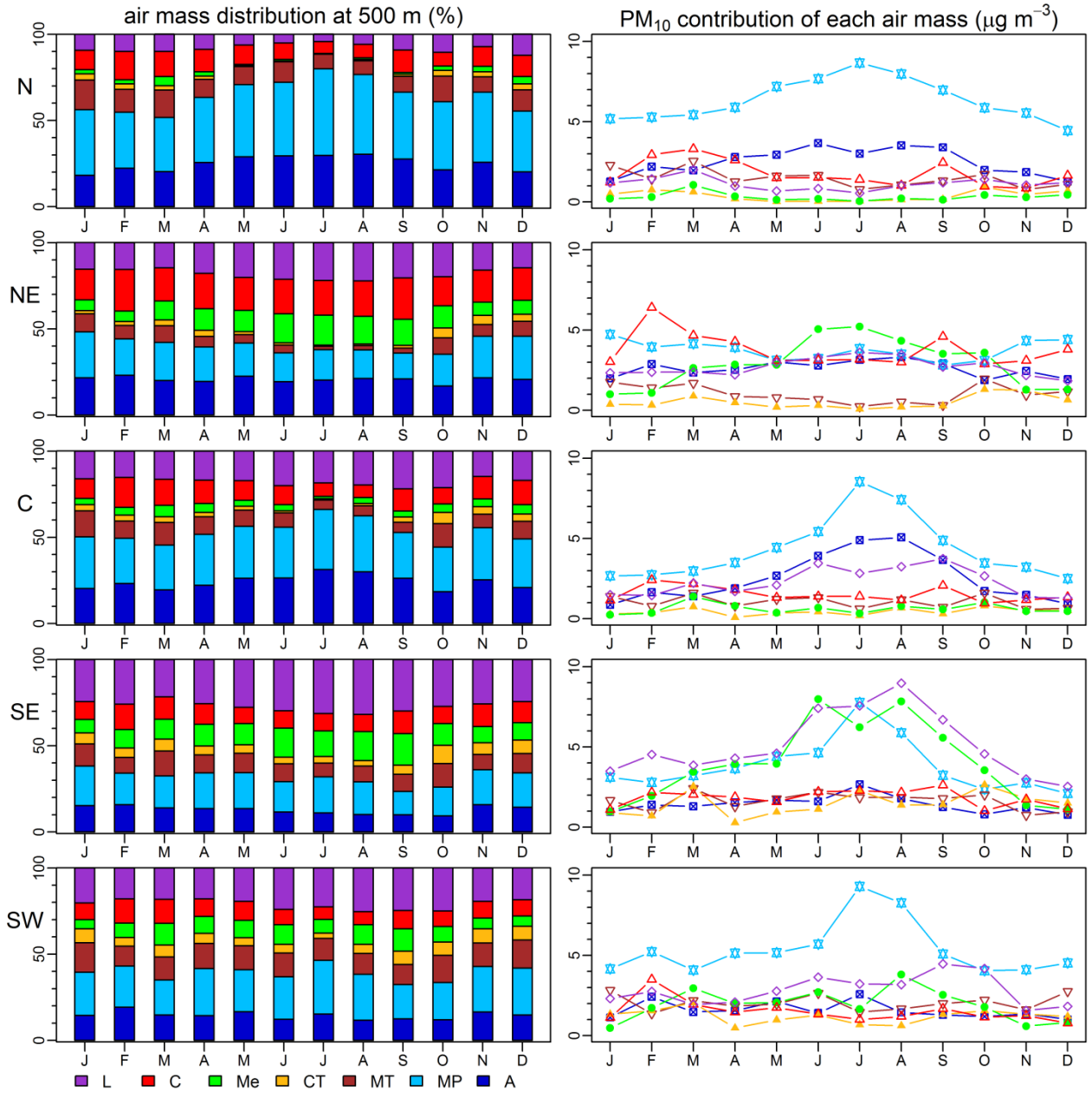

Figure 4. Frequency distribution of seven air masses in the five Iberian sectors at 500 m (left panels) and PM_{10} contribution of each air mass (right panels): L (local), C (continental), Me (Mediterranean), CT (continental tropical), MT (tropical maritime), MP (polar maritime), and A (Arctic).

Figure 5

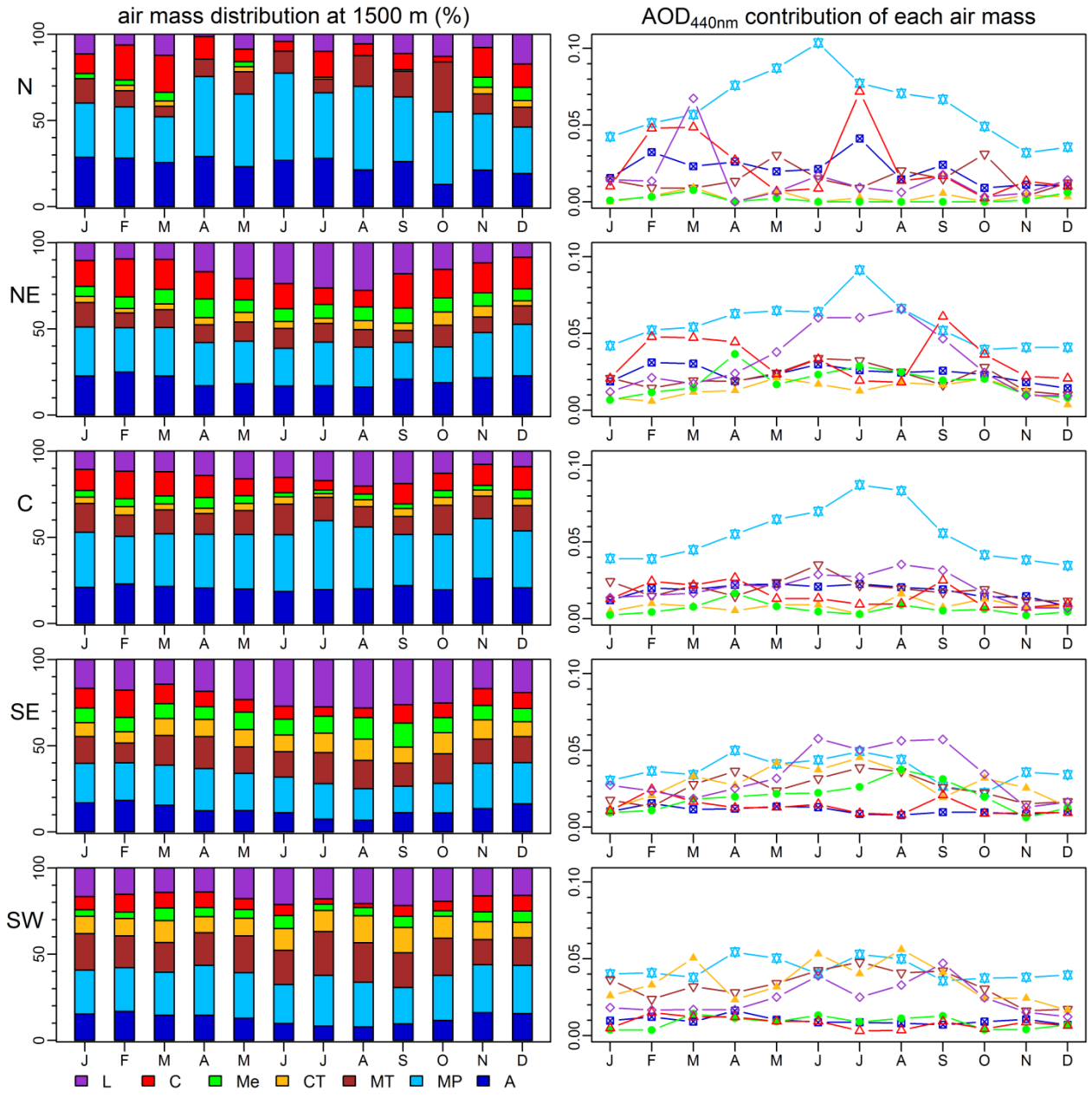

Figure 5. Frequency distribution of seven air masses in the five Iberian sectors at 1500 m (left panels) and AOD_{440nm} contribution of each air mass (right panels): L (local), C (continental), Me (Mediterranean), CT (continental tropical), MT (tropical maritime), MP (polar maritime), and A (Arctic).

Figure 6

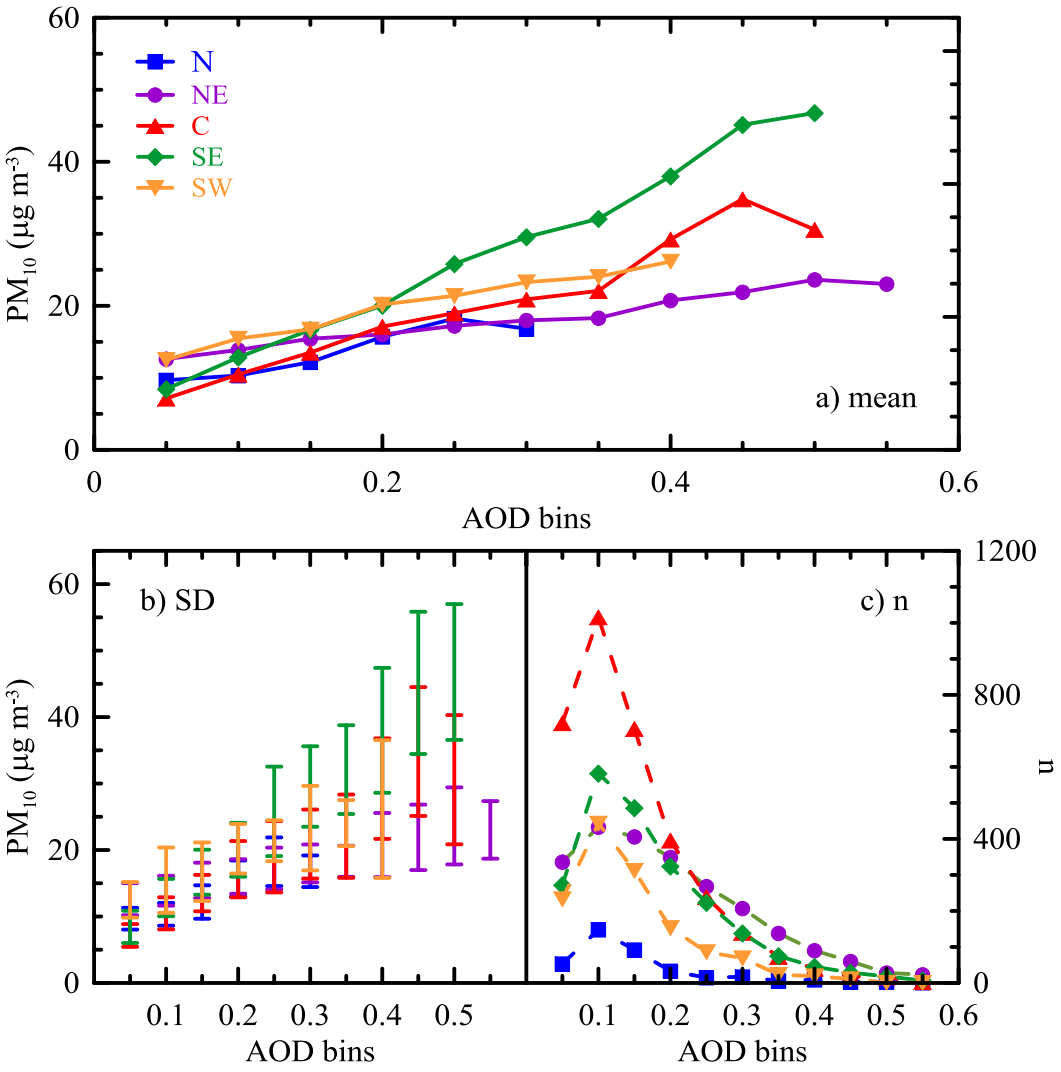

Figure 6. Mean (a), standard deviation (b), SD, and number of data (c), n, of daily PM_{10} concentration in AOD bins of width 0.05 in the five Iberian sectors.

Figure 7

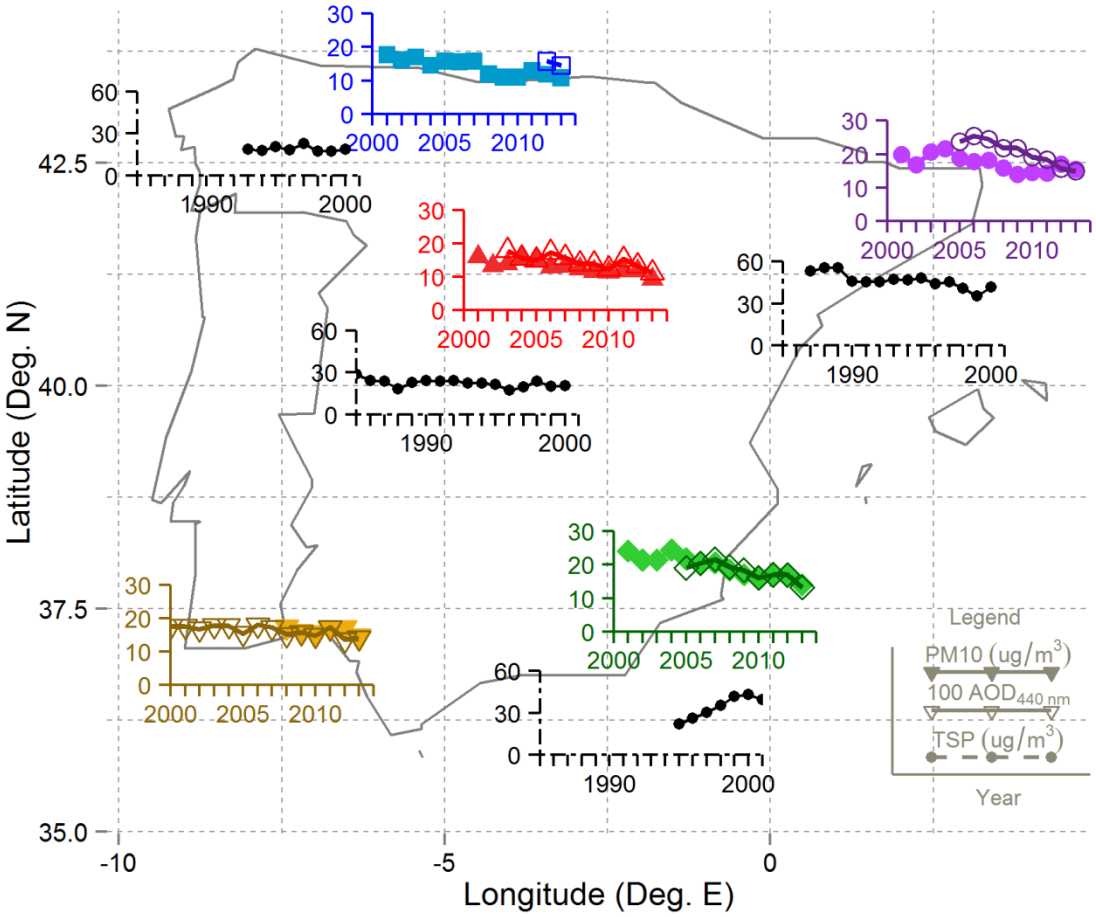

Figure 7. Yearly values of PM_{10} (solid symbols & solid axes), AOD_{440nm} (open symbols & solid axes), and TSP (black circles & dashed axes) in the five Iberian sectors.

Figure 8

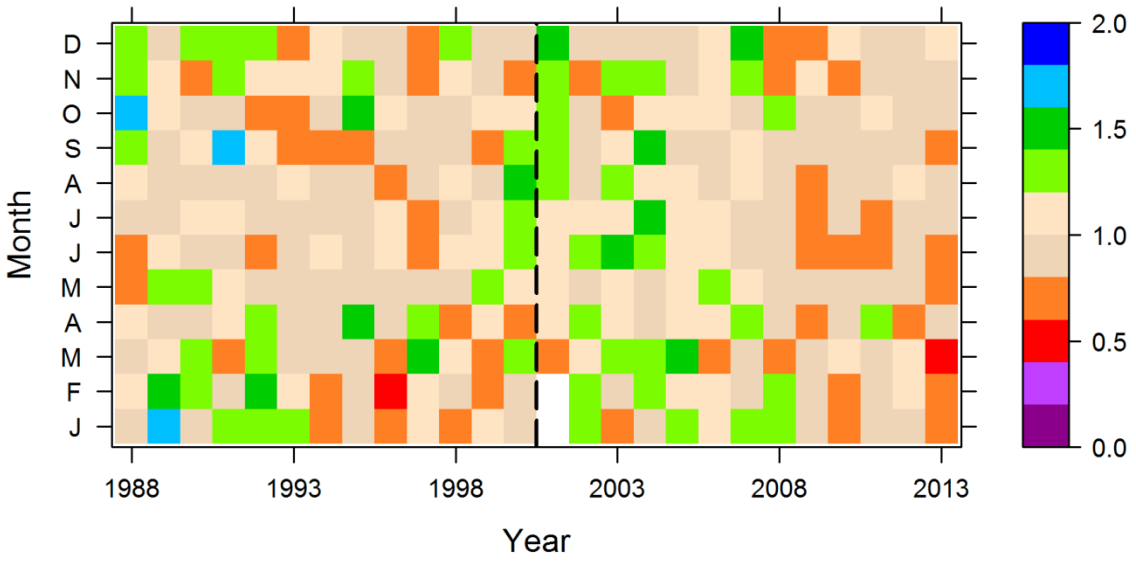

Figure 8. Time series of the ratio between the actual TSP or PM_{10} data and the corresponding monthly climatological mean using the average time series in Spain between 1987 and 2013. Vertical dashed line points out the separation between TSP (before 2001) and PM_{10} (beyond 2001) data.

SUPLEMENTARY MATERIAL

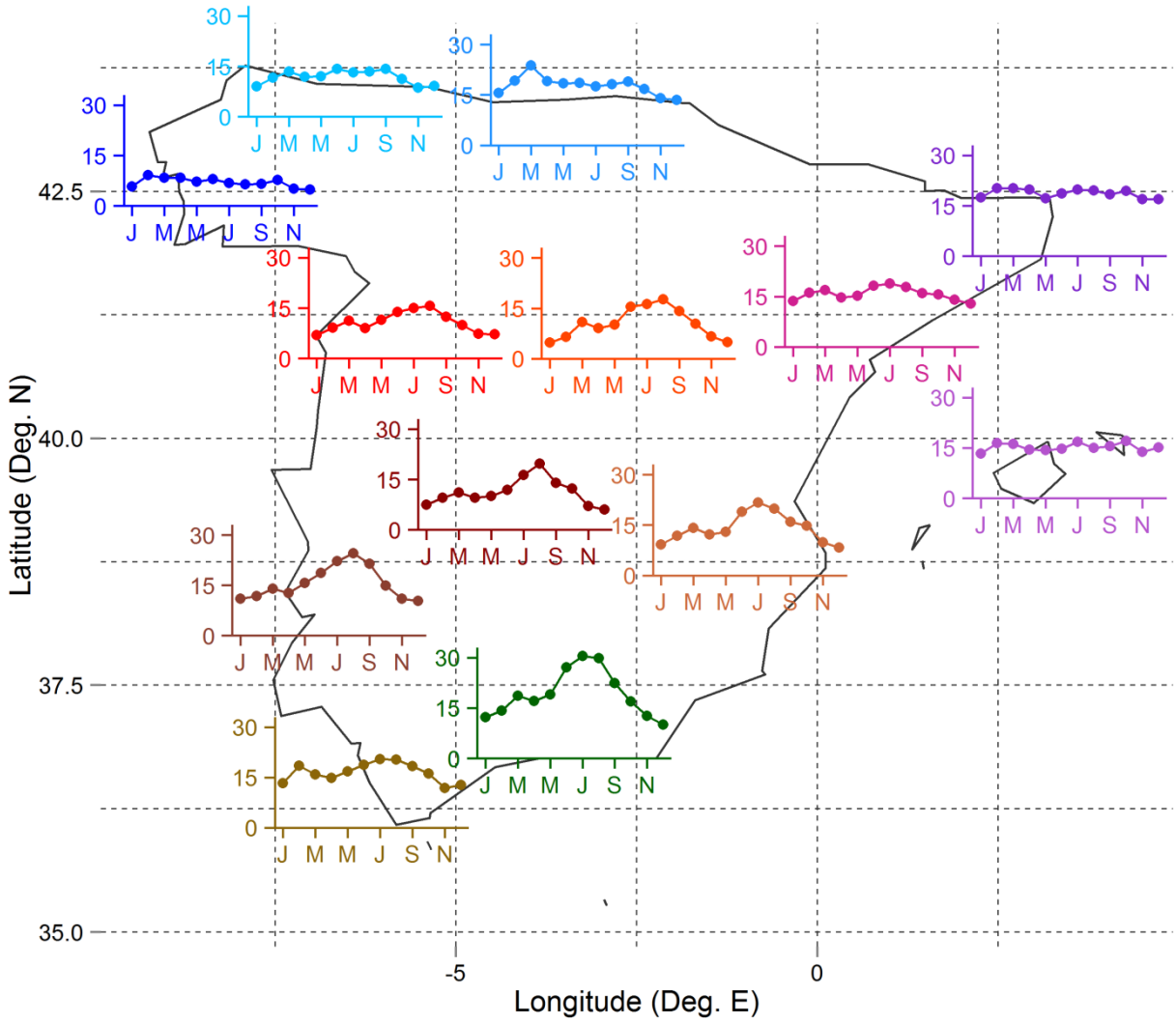

Figure S1. PM_{10} annual cycle (µg m^{-3}) in the 13 EMEP sites in the Iberian Peninsula.

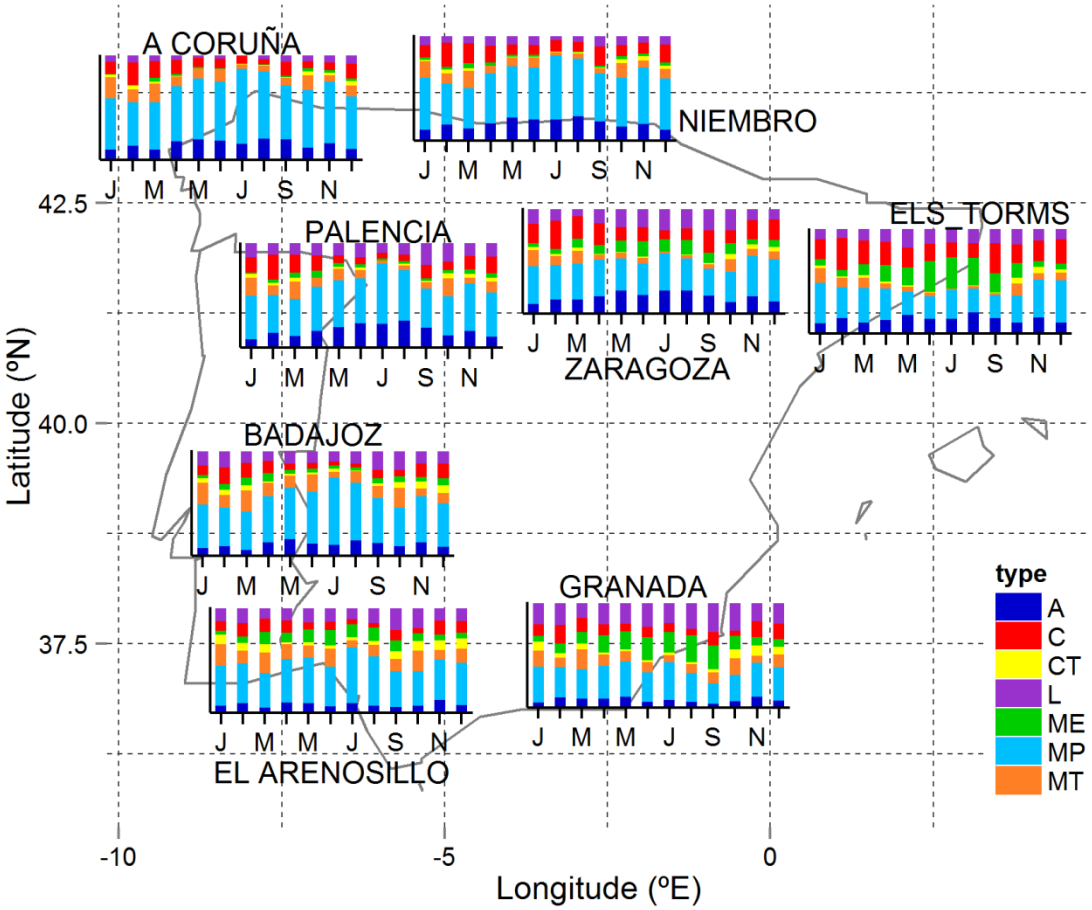

Figure S2. Relative frequency of the seven air mass types at 500m in 8 sites used in this study.

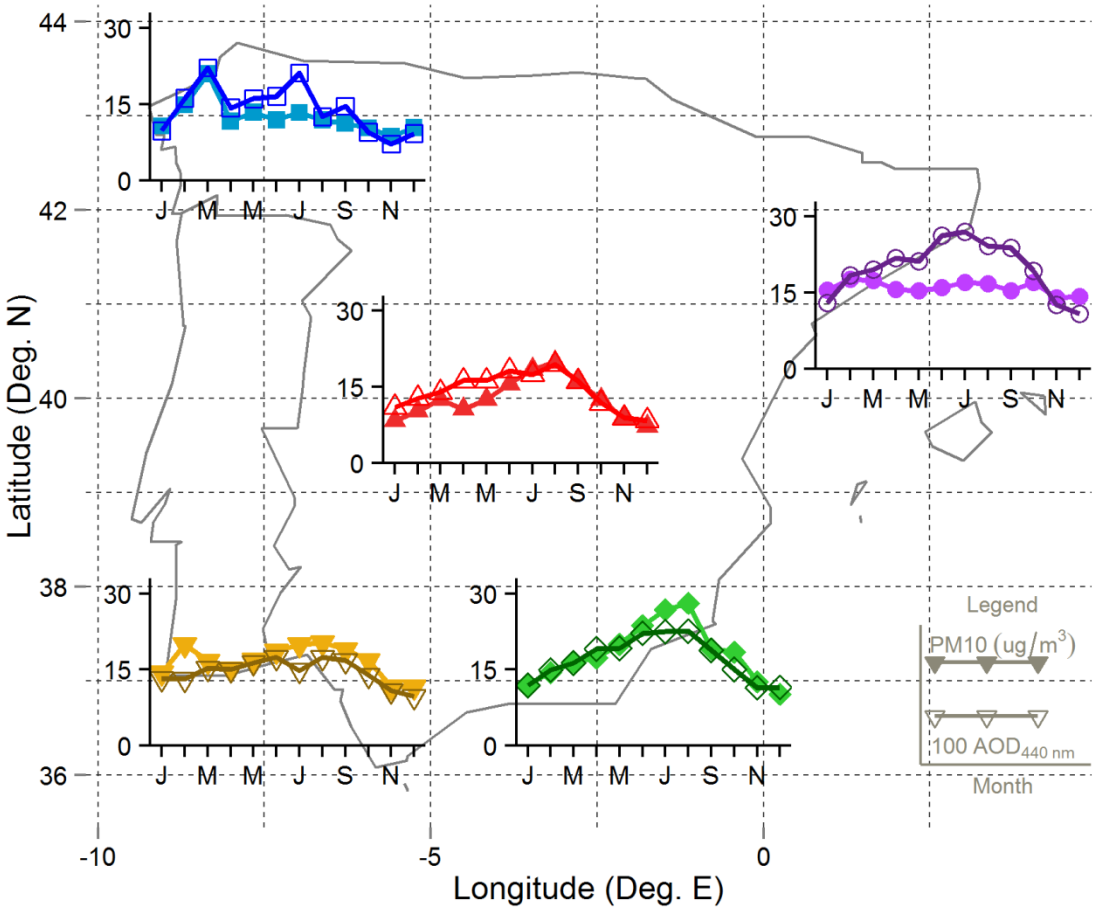

Figure S3. PM_{10} and AOD_{440nm} annual cycles considering only those days with simultaneous data of both variables.